Theory of GISAXS

Zhang Jiang

zjiang@aps.anl.gov

Advanced Photon Source

Argonne National Laboratory

2014.05.24 ACA GISAXS Workshop

A few good references

- Books:
  - Elements of modern x-ray physics, Jens Als-Nielsen and Des Mcmorrow
  - X-Ray Scattering from Soft-Matter Thin Films, Metin Tolan (e-library)
  - X-Ray Diffuse Scattering from Self-Organized Mesoscopic Semiconductor Structures, Martin Schmidbauer (e-library)

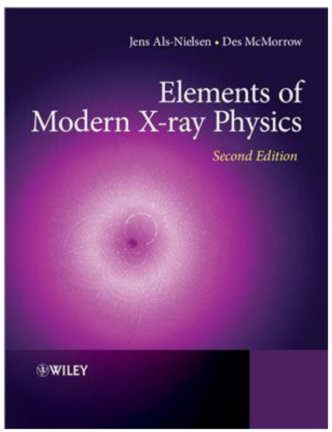

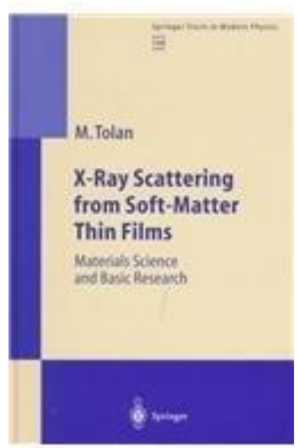

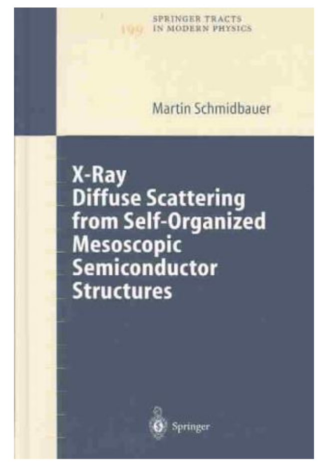

- Review article
  - Probing surface and interface morphology with grazing incidence small angle x-ray scattering, Renaud et al., Surf. Sci. Rep. 64, 255 (2009)

GISAXS = GI+SAXS
(Grazing Incidence Small Angle X-ray Scattering)

SAXS

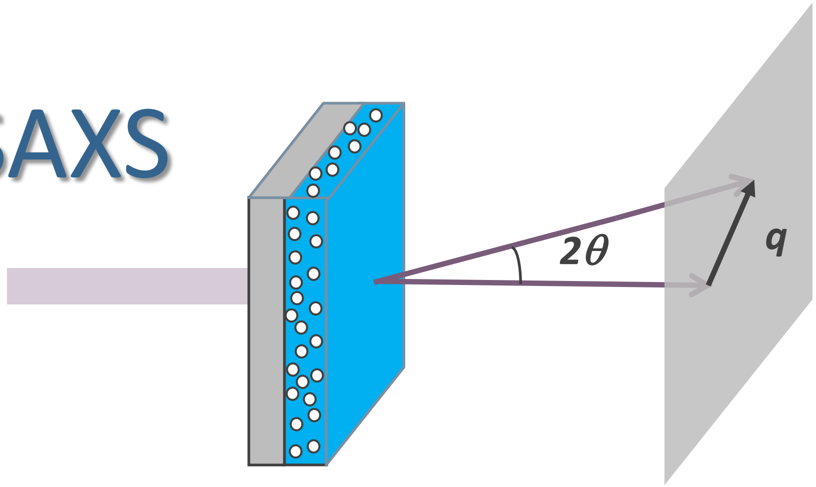

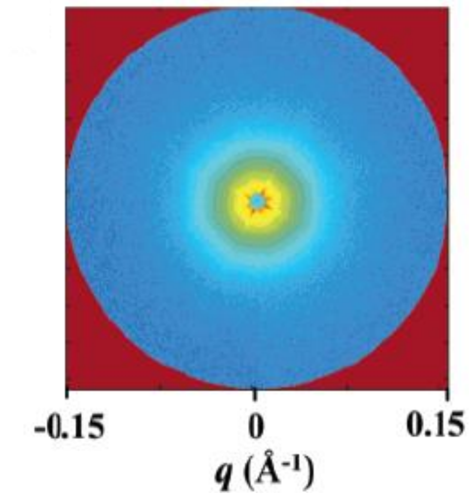

GISAXS

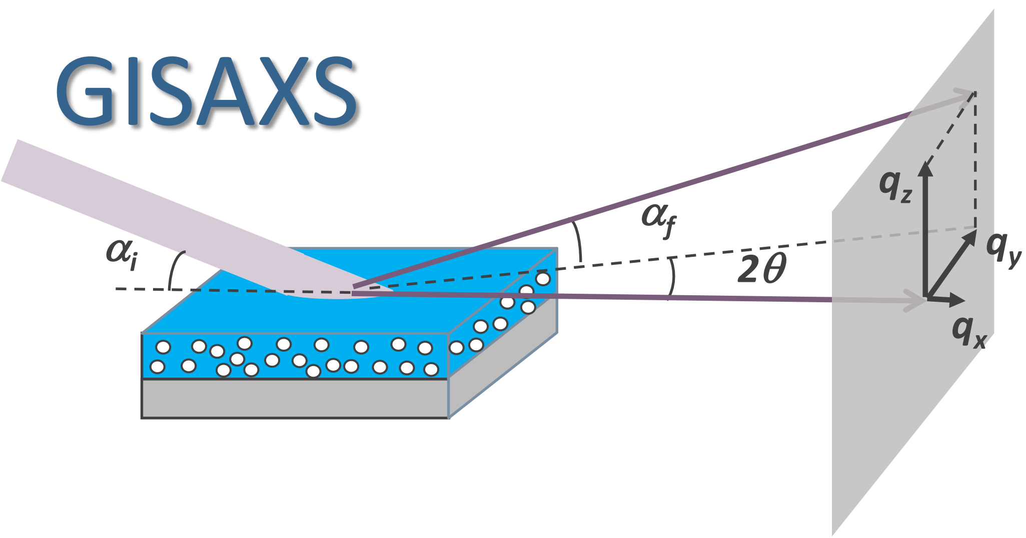

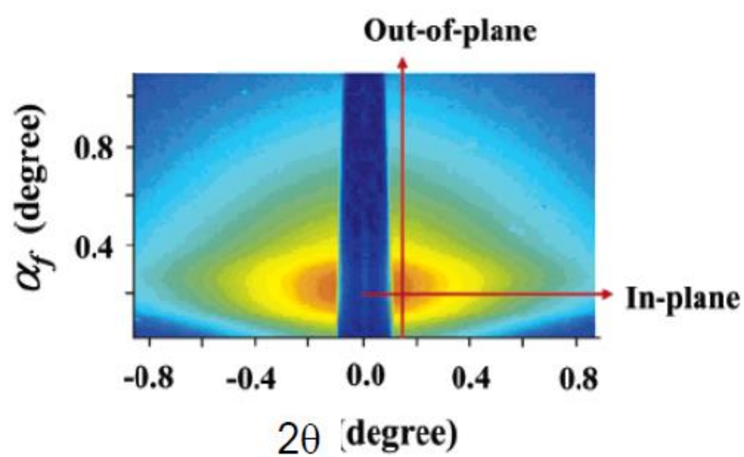

Grazing-incidence x-ray scattering (GIXS) geometry

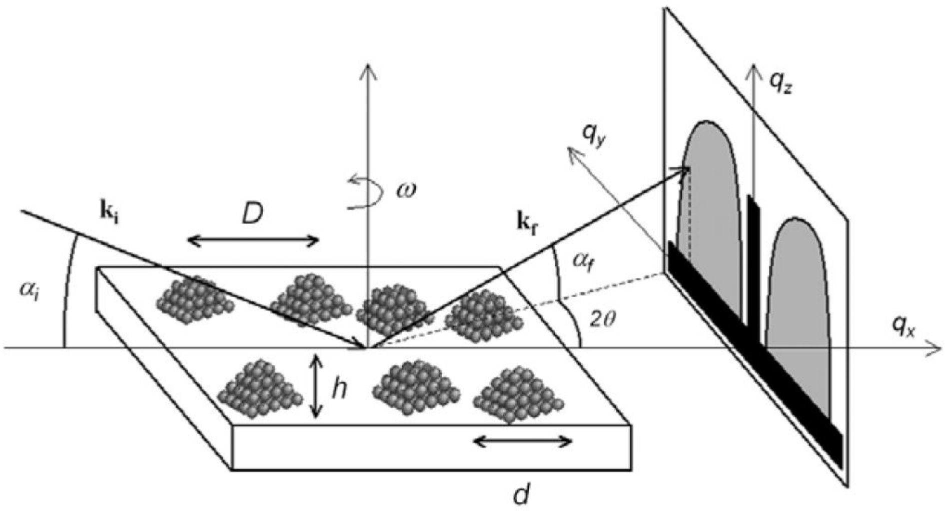

Wave vector transfer in sample reference frame:

$$q = \begin{pmatrix} q_x \\ q_y \\ q_z \end{pmatrix} = \frac{2\pi}{\lambda} \begin{pmatrix} \cos(\alpha_f)\cos(2\theta) - \cos(\alpha_i) \\ \cos(\alpha_f)\sin(2\theta) \\ \sin(\alpha_f) + \sin(\alpha_i) \end{pmatrix}$$

True q (for the scattering/diffraction) will be different due to reflection and refraction effects.

- Grazing-incidence small-angle x-ray scattering (GISAXS) — for structures > 1nm
- Grazing-incidence wide-angle x-ray scattering (GIWAXS) or Grazing-incidence x-ray diffraction (GIXD) — for structures < 1nm, typically on atomic length scales
- X-ray reflectivity — averaged structures normal to surface like thickness and roughness
- In GIXS, horizontal linecut (along q_y) and vertical linecut (along q_z) are often used for data analysis

Reflection and refraction

Index of refraction

$$n \geq 1$$

$$n = 1 - \delta + i\beta$$

$$n \approx 1 - \frac{\lambda^2}{2\pi} r_e \rho + i \frac{\lambda}{4\pi} \mu$$

$$0 < \mathrm{Real}[n] \leq 1$$

Light

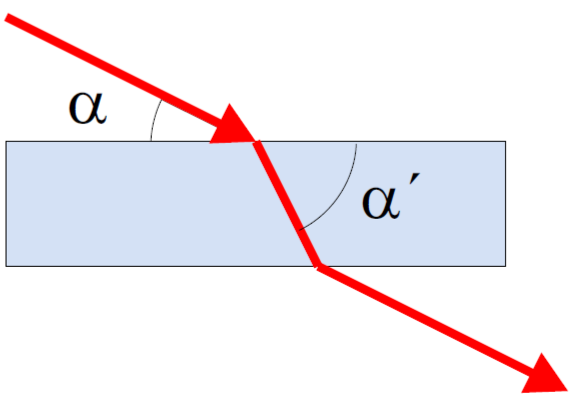

X-rays

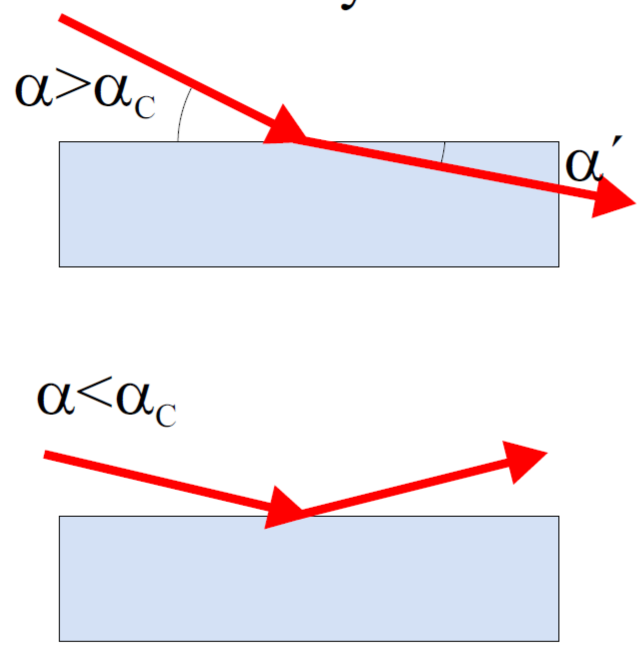

Total external reflection

Reflection and refraction

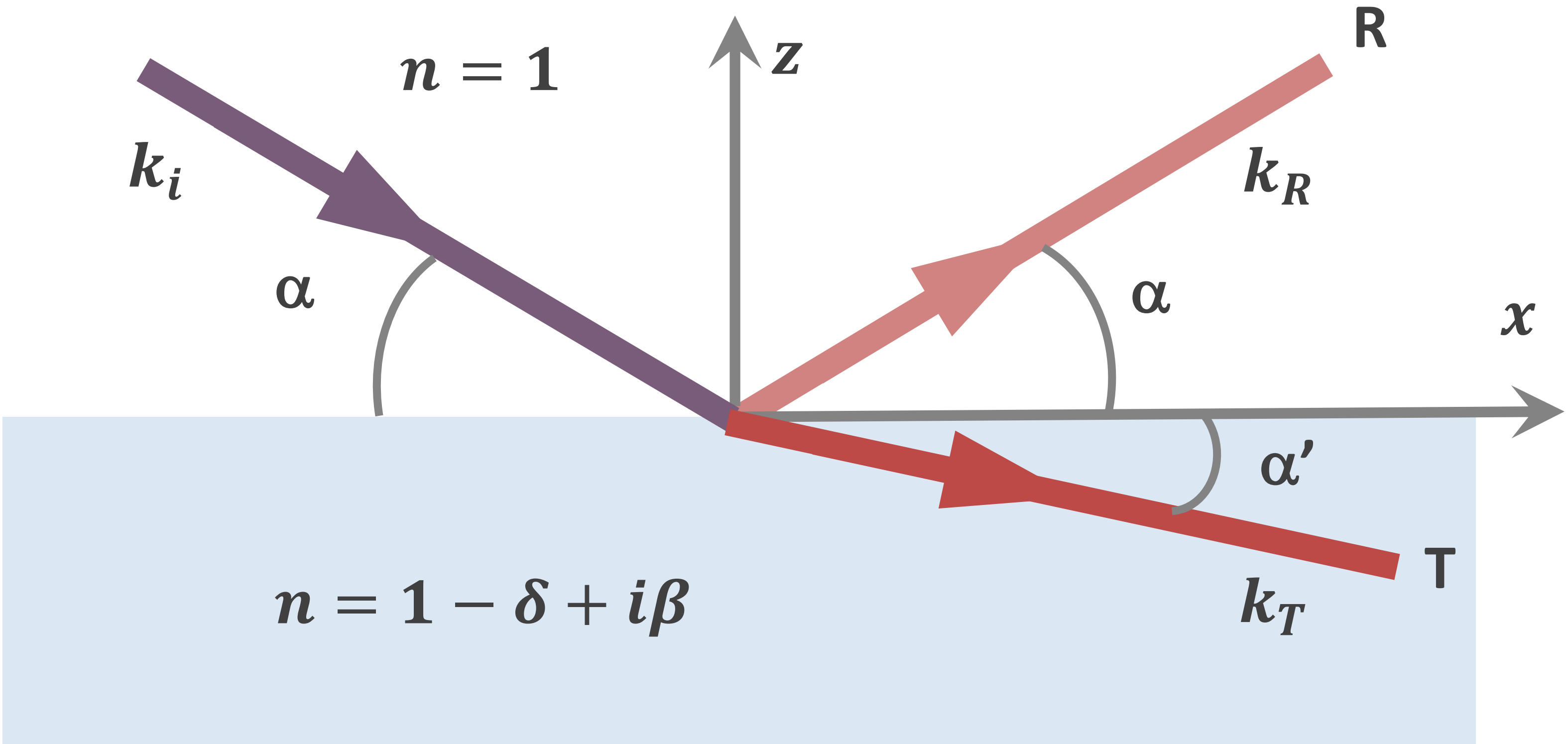

Snell's law: $\cos\alpha = n\cos\alpha'$

Critical angle for total external reflection (α'=0): $\alpha_c = \cos^{-1} n \approx \sqrt{2\delta}$

Typical $\delta \sim 10^{-5}$, so $\alpha_c \sim 0.1° - 0.5°$

Wave vector transfer for reflected beam $q_z = 2k sin(\alpha)$

Evanescent wave and penetration depth

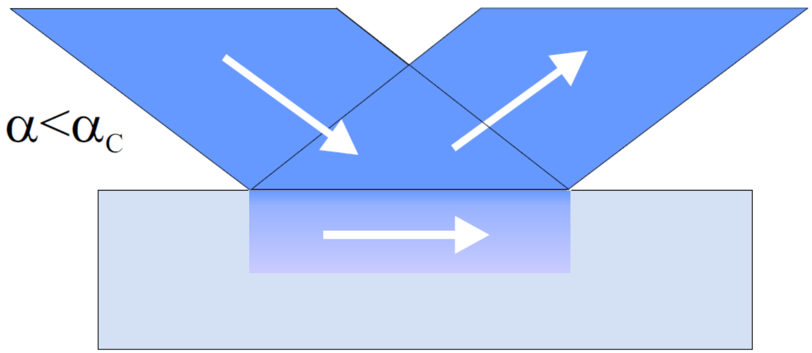

Penetration depth on Si surface with λ=1.54A

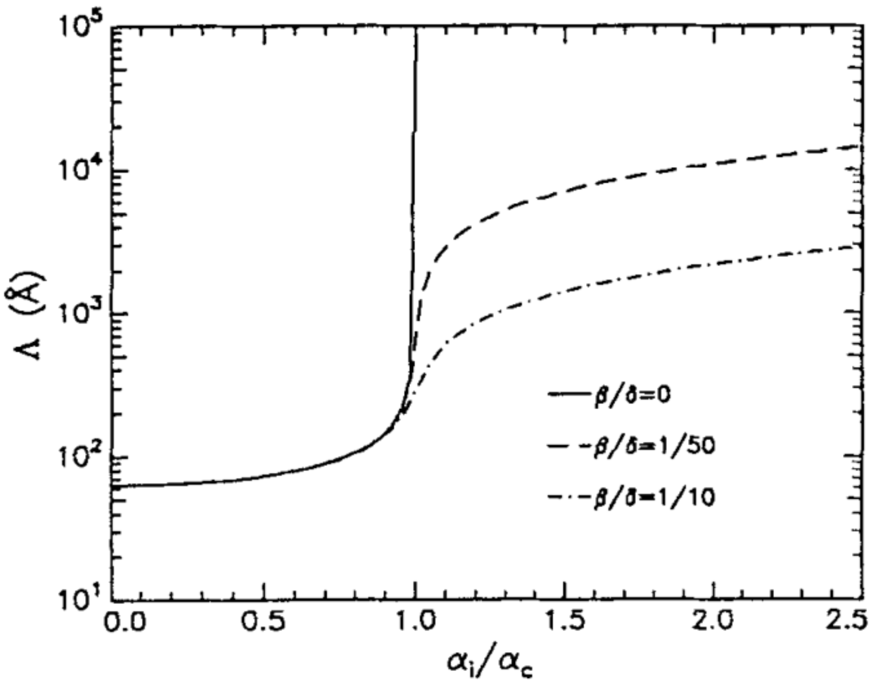

- The reflection is almost 100%, and x-ray only penetrates a typical depth of a few nanometer.
- By tuning the incident angle, x-ray can be a *surface* sensitive technique

Reflection and transmission coefficients

Electric fields $$E(\boldsymbol{r},\boldsymbol{k}) = E_0 e^{-i\boldsymbol{k}_{||}\cdot\boldsymbol{r}_{||}} \begin{cases} e^{-ik_{i,z}z} + r e^{ik_{i,z}z} & \text{for } z > 0 \\ t e^{-ik_{t,z}z} & \text{for } z < 0 \end{cases}$$

Boundary condition
& Snell's law

Reflection and transmission coefficients (Fresnel formulas):

$$\begin{cases} r = \dfrac{k_{i,z} - k_{t,z}}{k_{i,z} + k_{t,z}} \\[2ex] t = \dfrac{2k_{t,z}}{k_{i,z} + k_{t,z}} \end{cases}$$

$R_F = |r|^2$ Fresnel reflectivity

$T_F = |t|^2$ Fresnel transmission

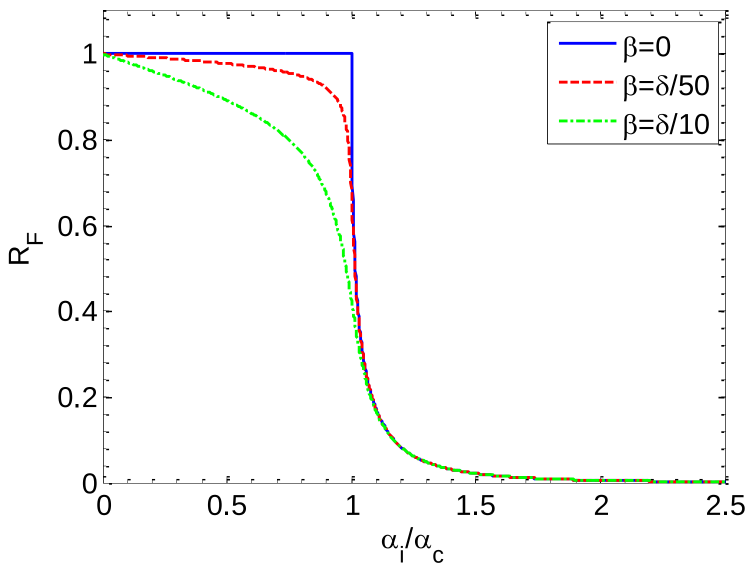

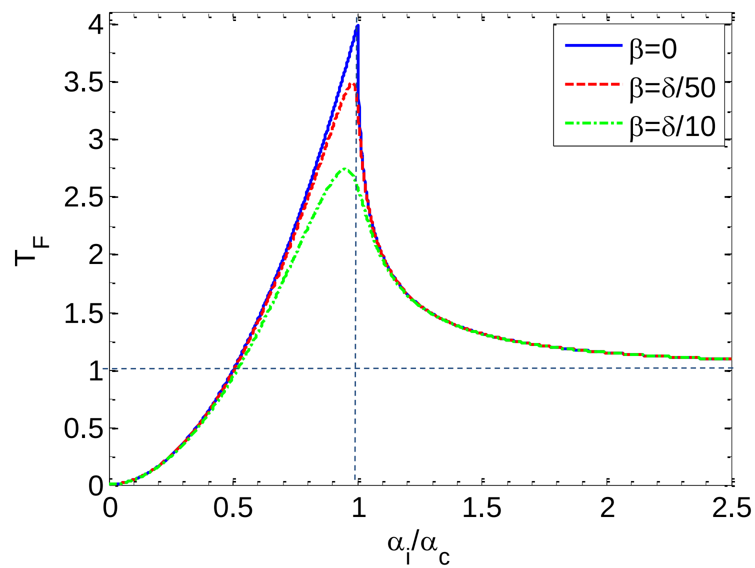

With n~1 for x-rays, in practice there is no difference between s- and p-polarizations.

Perfect & Imperfect „Mirrors“

Single rough surface

Height-height correlation

$$C(R) = \langle \delta z(0)\delta z(R) \rangle$$

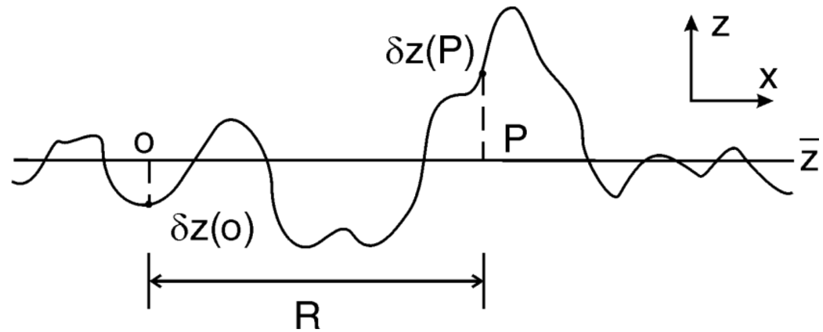

Distorted Wave Born Appximation

$$\left(\frac{d\sigma}{d\Omega}\right)_{\mathrm{diff}} = A r_e^2 |\Delta\rho|^2 |t(\alpha_i)|^2 \boxed{\left|t(\alpha_f)\right|^2} \frac{e^{-\frac{1}{2}\left[(q_{z,t})^2 + (q_{z,t}^*)^2\right]\sigma^2}}{\left|q_{z,t}\right|^2}$$

$$\times \int d\boldsymbol{R} \left[e^{\left|q_{z,t}\right|^2 C(R)} - 1 \right] e^{-i\boldsymbol{q}_{||}\cdot\boldsymbol{R}}$$

Born Approximation

$$\left(\frac{d\sigma}{d\Omega}\right)_{\mathrm{diff}} = A r_e^2 |\Delta\rho|^2 e^{-q_z^2\sigma^2} \int d\boldsymbol{R}\left[e^{q_z^2 C(R)} - 1\right] e^{-i\boldsymbol{q}_{||}\cdot\boldsymbol{R}}$$

GISAXS from silicon surface

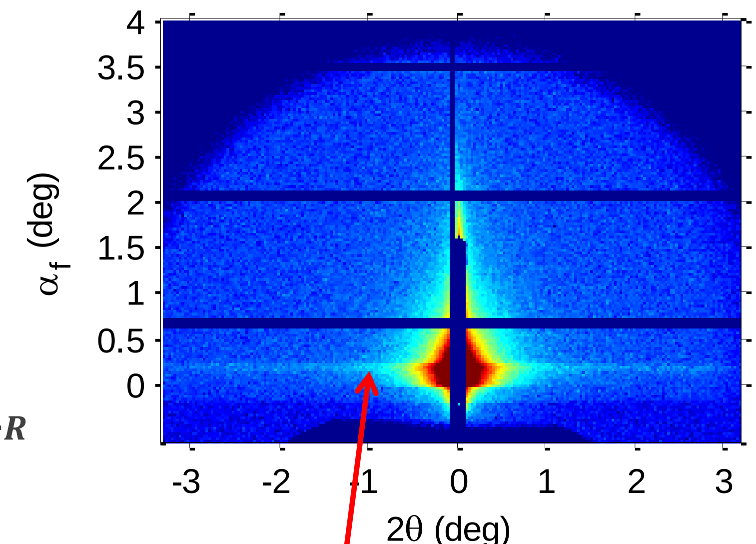

$\alpha_f = \alpha_c$

Yoneda peak

S. K. Sinha et al., PRB 38, 2297 (1988)

Kinematical vs. dynamical scattering

- In kinematical theory, i.e. Born approximation (BA), as employed in SAXS data analysis, the magnitude of the x-ray electric field does not change over the x-ray path and multiple scattering is ignored.
- For grazing-incidence scattering, the electric field intensity normal to the surface is redistributed. This leads to
  - incident wave amplitude varies at different height on surface
  - much higher chance that the scattered beam will be re-scattered again (this in fact leads to the total external reflection)
- Distorted Wave Born approximation (DWBA) is developed to account for these dynamical phenomena.

Theoretical background

The wave propagation equation in medium can be obtained from Maxwell equation. This equation is in general called Helmholtz equation:

$$(\nabla^2 + n^2(\boldsymbol{r})k^2)\psi(\boldsymbol{r}) = 0 \qquad \text{with } n(\boldsymbol{r}) = 1 - \delta = 1 - \frac{r_e \rho(\boldsymbol{r})\lambda^2}{2\pi}$$

Kinematical approximation

$$\psi(\boldsymbol{r}) \approx \boxed{e^{i\boldsymbol{k}\cdot\boldsymbol{r}}} + \boxed{\frac{e^{ikr}}{r} f(\theta, \varphi)}$$

Incident wave

Outgoing wave

$$\frac{d\sigma}{d\Omega} = |f(\theta,\varphi)|^2 = r_e^2 \underbrace{\left| \int d\boldsymbol{r}\rho(\boldsymbol{r})e^{-i\boldsymbol{q}\cdot\boldsymbol{r}} \right|^2}_{\text{Form factor}}$$

See Jackson's text book *Classical Electrodynamics* for details of solving Helmholtz equation

Dynamical approximation

$$n^2(\mathbf{r}) = n_0^2(\mathbf{r}) + \delta n^2(\mathbf{r})$$

- Surface structure, such as nanocrystals and roughness, is treated as small perturbation to a known reference (unperturbed) state.
- This reference state is the Fresnel wave-field for an idea surface (step-like and no roughness).
- This approximation is called distorted wave Born approximation (DWBA)

DWBA - for a single interface: unperturbed state

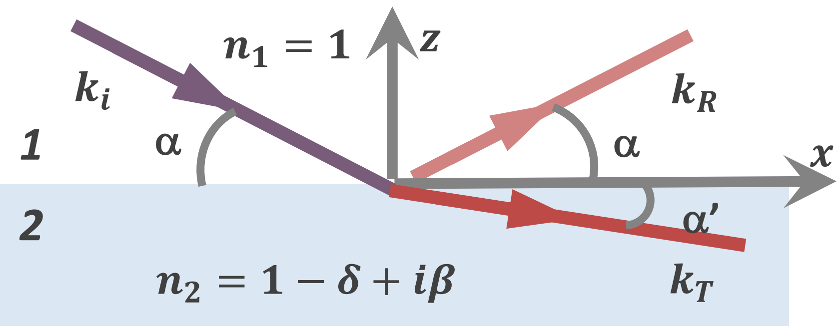

Incident beam

$$\phi_0(\boldsymbol{r}, \boldsymbol{k}) = e^{i\boldsymbol{k}_{||}\cdot\boldsymbol{r}_{||}} e^{-ik_{1z}z}$$

Initial state:

$$\psi_i(\boldsymbol{r}, \boldsymbol{k}) = e^{i\boldsymbol{k}_{||}\cdot\boldsymbol{r}_{||}} \begin{cases} e^{-ik_{i,1z}z} + r e^{ik_{i,1z}z} & \text{for } z > 0 \\ t e^{-ik_{i,2z}z} & \text{for } z < 0 \end{cases}$$

Time reversed state:

$$\psi_f^*(\boldsymbol{r}, \boldsymbol{k}) = e^{i\boldsymbol{k}_{||}\cdot\boldsymbol{r}_{||}} \begin{cases} e^{-ik_{f,1z}^*z} + r^* e^{ik_{f,1z}^*z} & \text{for } z > 0 \\ t^* e^{-ik_{f,2z}^*z} & \text{for } z < 0 \end{cases}$$

- $\psi_i(\boldsymbol{r}, \boldsymbol{k})$ and $\psi_f^*(\boldsymbol{r}, \boldsymbol{k})$ are unperturbed solutions corresponding to an ideal interface with sharp step-like profile:

$$(\nabla^2 + n_0^2(z)k^2)\psi(z) = 0 \qquad \text{where } n_0(z) \text{ is constant} \begin{cases} 1 \text{ for z} > 0 \\ n_2 \text{ for z} < 0 \end{cases}$$

- This unperturbed Helmholtz equation is then solved by calculating the Fresnel coefficients!

Perturbation theory and differential scattering cross section

Transition matrix T between states k_i and k_f is given by

$$\langle f|T|i\rangle \approx \langle \psi_f^*|n_0^2|\phi_i\rangle + \langle \psi_f^*|\delta n^2|\psi_i\rangle$$

See *Quantum Mechanics* by Schiff (1968)

In quantum mechanics, when an eigenstate changes to another due to a perturbation, Fermi golden rule is used to calculate its transition rate, i.e., the total differential scattering cross section:

$$\frac{d\sigma}{d\Omega} \sim \langle f|T|i\rangle$$

Dropping the specular part (i.e. $q_{||} = 0$), the non-specular part for objects in medium 1 (often vacuum) is then given by

$$\left(\frac{d\sigma}{d\Omega}\right)_{\mathrm{diff}} = r_e^2 \left| \begin{array}{l} \displaystyle\int \rho(\boldsymbol{r}) e^{-i\boldsymbol{q}_{||}\cdot\boldsymbol{r}_{||}} e^{-i\boxed{\left(k_z^f - k_z^i\right)}z} d\boldsymbol{r} + \boxed{r(\alpha_f)} \int \rho(\boldsymbol{r}) e^{-i\boldsymbol{q}_{||}\cdot\boldsymbol{r}_{||}} e^{-i\boxed{\left(-k_z^f - k_z^i\right)}z} d\boldsymbol{r} \\ + \boxed{r(\alpha_i)} \displaystyle\int \rho(\boldsymbol{r}) e^{-i\boldsymbol{q}_{||}\cdot\boldsymbol{r}_{||}} e^{-i\boxed{\left(k_z^f + k_z^i\right)}z} d\boldsymbol{r} + \boxed{r(\alpha_f) r(\alpha_i)} \int \rho(\boldsymbol{r}) e^{-i\boldsymbol{q}_{||}\cdot\boldsymbol{r}_{||}} e^{-i\boxed{\left(-k_z^f + k_z^i\right)}z} d\boldsymbol{r} \end{array} \right|^2$$

$\rho(\boldsymbol{r})$ is the electron density of the perturbations, e.g., supported nanocrystals

Supported nano-objects

$$\left(\frac{d\sigma}{d\Omega}\right)_{\text{diff}} = r_e^2|\Delta\rho|^2\left|\mathcal{F}\left(q_{||}, k_z^i, k_z^f\right)\right|^2$$

$$\mathcal{F}\left(q_{||}, k_z^i, k_z^f\right) = \boxed{F\left(q_{||}, q_z^1\right)} + \boxed{r\left(\alpha_f\right)F\left(q_{||}, q_z^2\right)} + \boxed{r(\alpha_i)F\left(q_{||}, q_z^3\right)} + \boxed{r(\alpha_i)r\left(\alpha_f\right)F\left(q_{||}, q_z^4\right)}$$

$$q_z^1 = k_z^f - k_z^i$$

$$q_z^2 = -k_z^f - k_z^i$$

$$q_z^3 = k_z^f + k_z^i$$

$$q_z^4 = -k_z^f + k_z^i$$

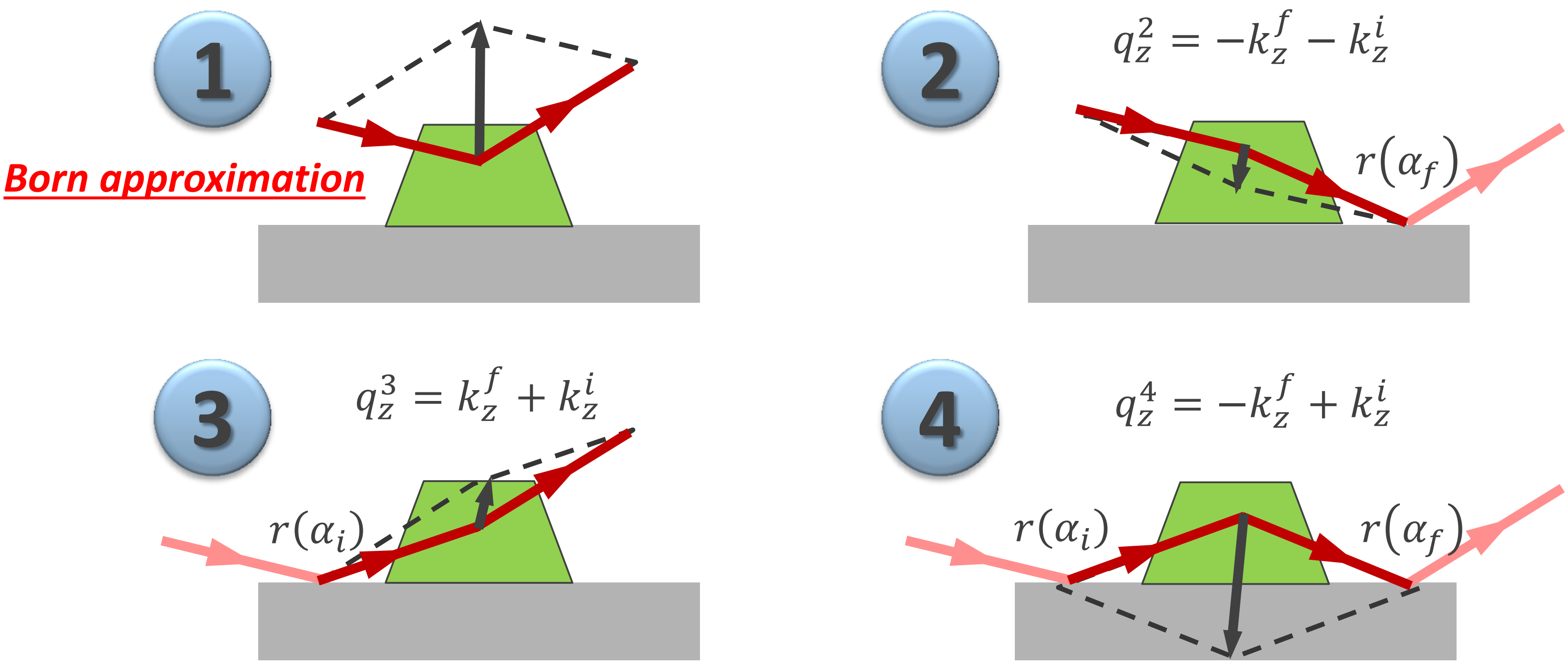

Supported nano-objects

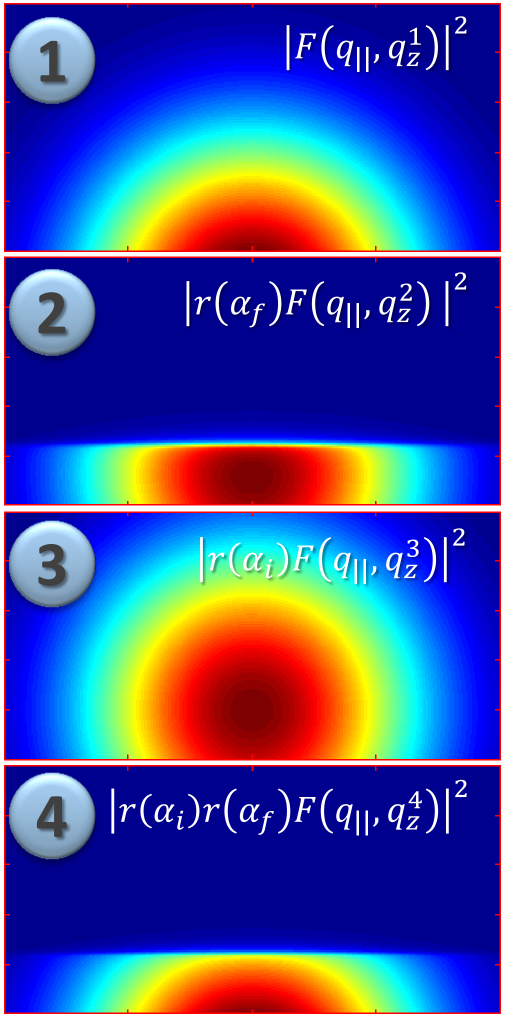

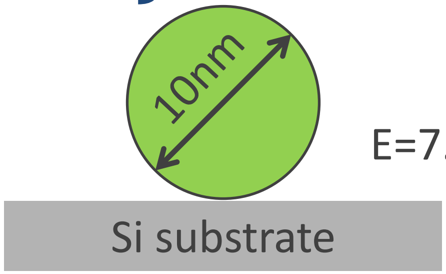

E=7.35 keV

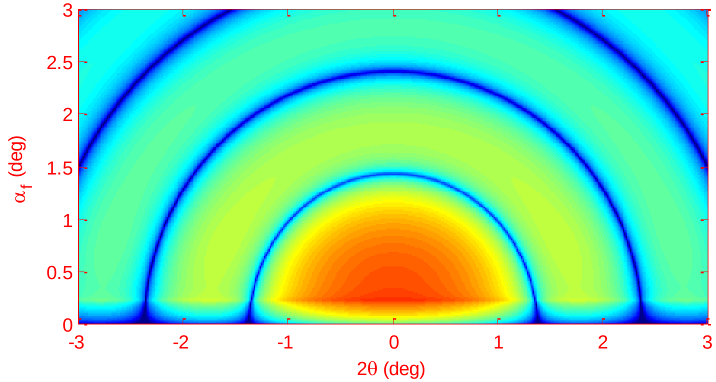

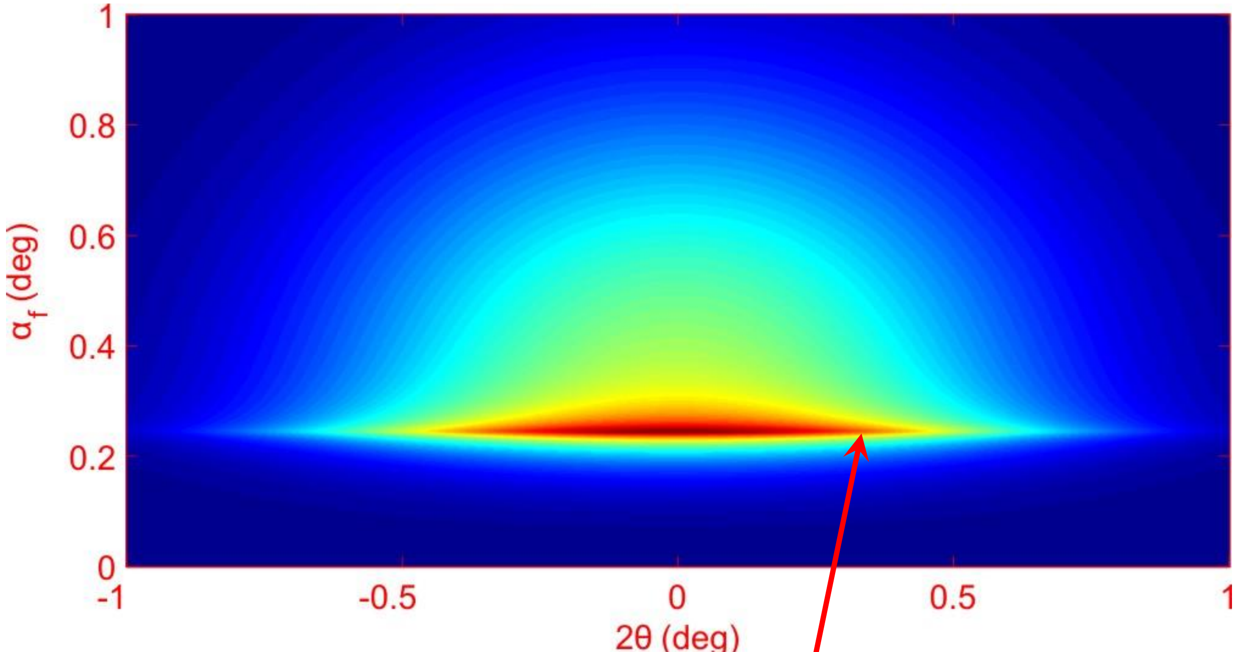

$\alpha_f = \alpha_c$ of silicon: Yoneda peak

Supported nano-objects: example

Epitaxy of Pd nano-islands
on MgO (001) substrate

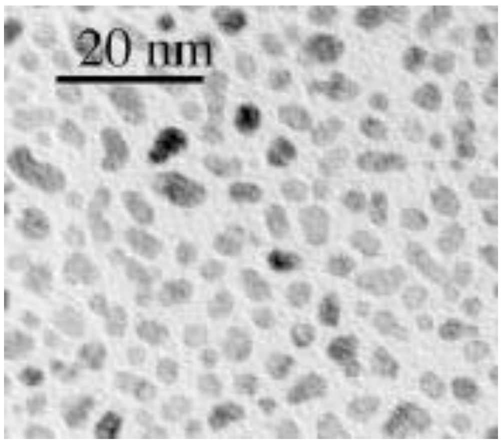

$$I \propto \left|\mathcal{F}\left(q_{||}, k_z^i, k_z^f\right)\right|^2 S\left(q_{||}, k_z^i, k_z^f\right)$$

- Form factor: disk
- Structure factor: 1D paracrystal

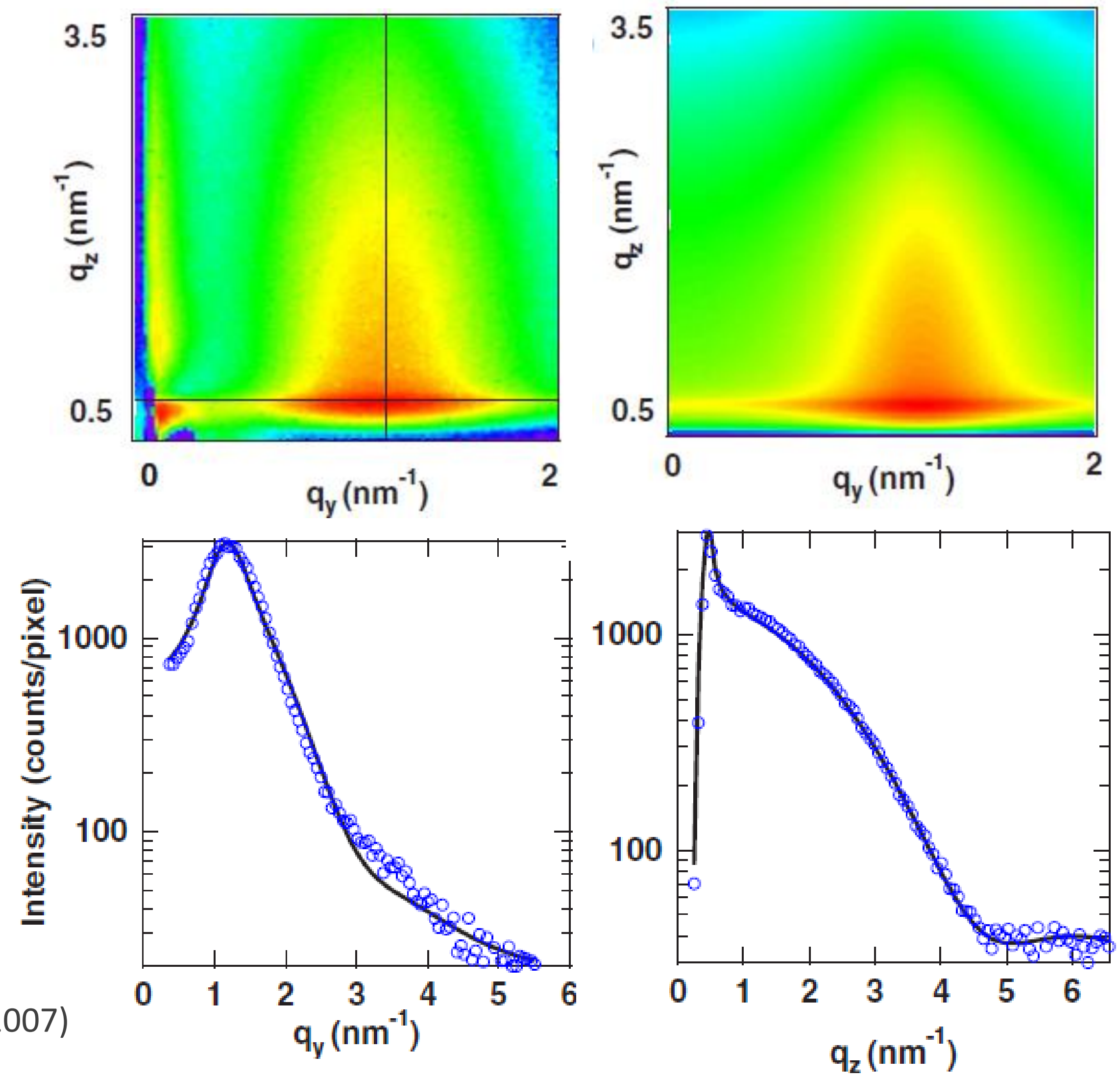

J. Olander, et al., PRB 76, 75409 (2007)
R. Lazzari, ISGISAXS software

Buried structures

$$\psi(\boldsymbol{r},\boldsymbol{k}) = e^{i\boldsymbol{k}_{||}\cdot\boldsymbol{r}_{||}}\begin{cases} e^{-ik_{z,1}z} + R_1 e^{ik_{z,1}z} & \text{for } z > 0 \\ T_2 e^{-ik_{z,2}z} + R_2 e^{ik_{z,2}z} & \text{for } -d < z < 0 \\ T_3 e^{-ik_{z,3}z} & \text{for } z < -d \end{cases}$$

$$\mathcal{F}\left(q_{||}, k_{z,1}^{i}, k_{z,1}^{f}\right) = \boxed{T_2\left(k_{z,2}^{f}\right)T_2\left(k_{z,2}^{i}\right)F\left(q_{||}, q_{z,2}^{1}\right)} + \boxed{R_2\left(k_{z,2}^{f}\right)T_2\left(k_{z,2}^{i}\right)F\left(q_{||}, q_{z,2}^{2}\right)}$$
$$+ \boxed{T_2\left(k_{z,2}^{f}\right)R_2\left(k_{z,2}^{i}\right)F\left(q_{||}, q_{z,2}^{3}\right)} + \boxed{R_2\left(k_{z,2}^{f}\right)R_2\left(k_{z,2}^{i}\right)F\left(q_{||}, q_{z,2}^{4}\right)}$$

1

$$q_{z,2}^{1} = k_{z,2}^{f} - k_{z.2}^{i}$$

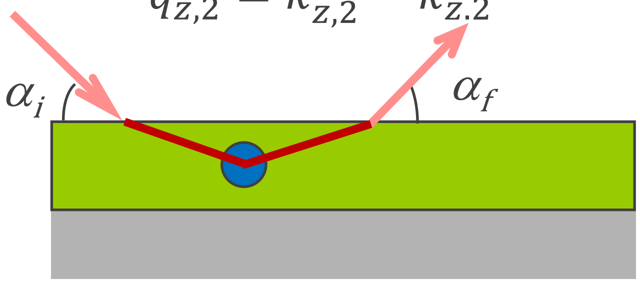

2

$$q_{z,2}^{2} = -k_{z,2}^{f} - k_{z.2}^{i}$$

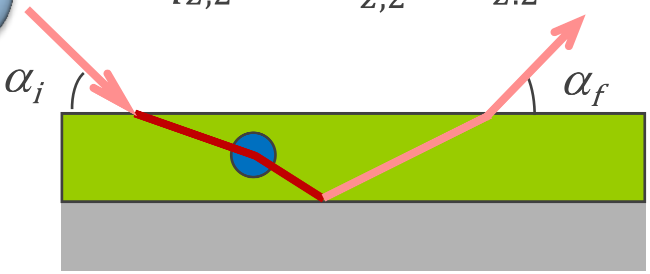

3

$$q_{z,2}^{3} = k_{z,2}^{f} + k_{z.2}^{i}$$

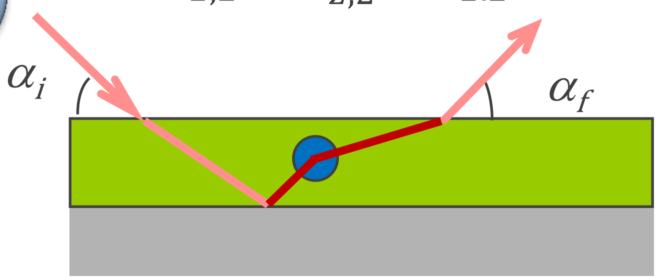

4

$$q_{z,2}^{4} = -k_{z,2}^{f} + k_{z.2}^{i}$$

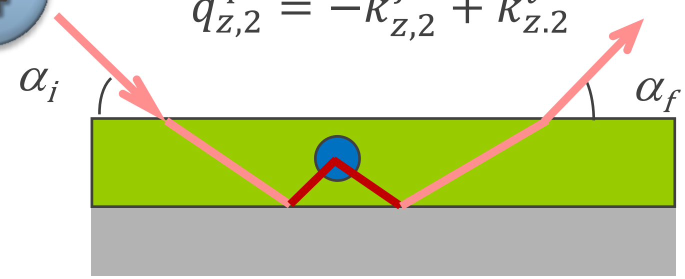

Transmission and reflection channels

1 2
$$\alpha_f = \arcsin\sqrt{\left(\frac{q_z}{k}\right)^2 + \sin^2\alpha_i - \frac{2q_z}{k}\sqrt{n^2 - 1 + \sin^2\alpha_i}}$$

3 4
$$\alpha_f = \arcsin\sqrt{\left(\frac{q_z}{k}\right)^2 + \sin^2\alpha_i + \frac{2q_z}{k}\sqrt{n^2 - 1 + \sin^2\alpha_i}}$$

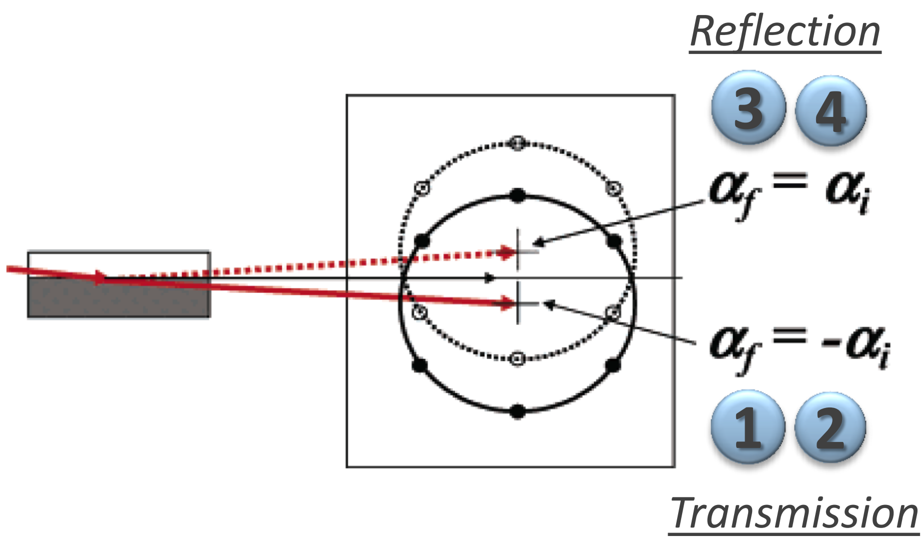

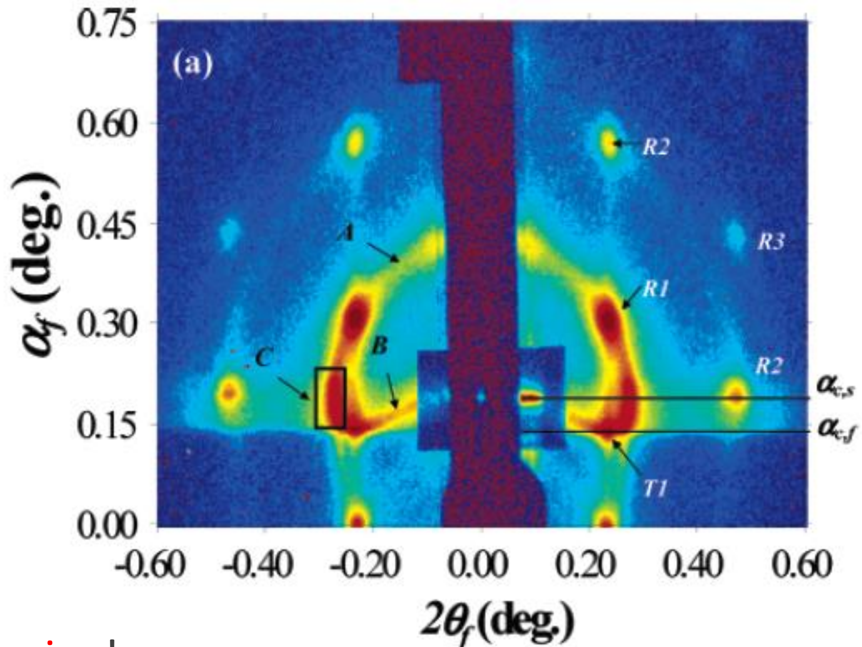

Important for substrate supported 3D structure indexing!

B. Lee et al, Macromolecules 38, 4316 (2005)

Near exit-side critical angle

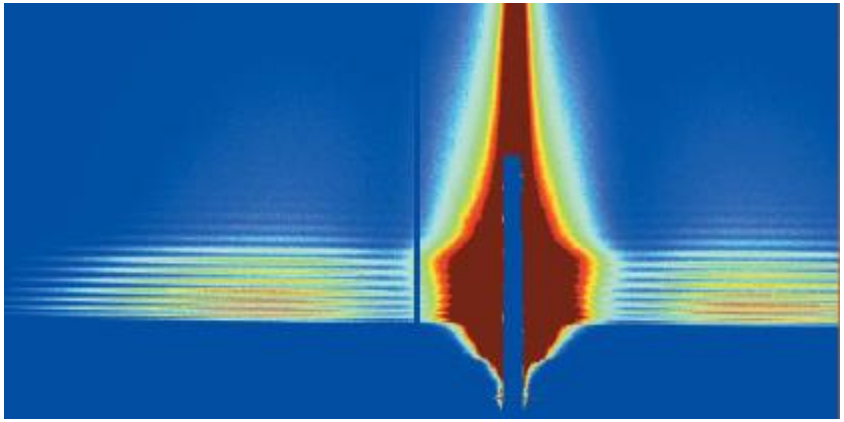

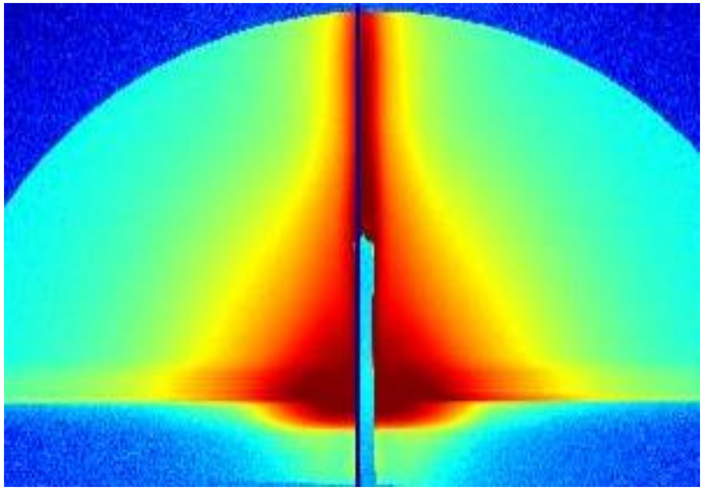

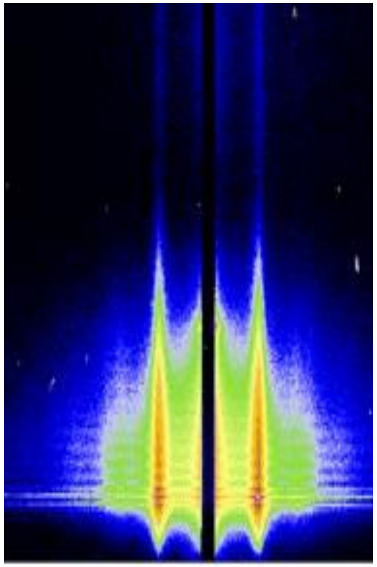

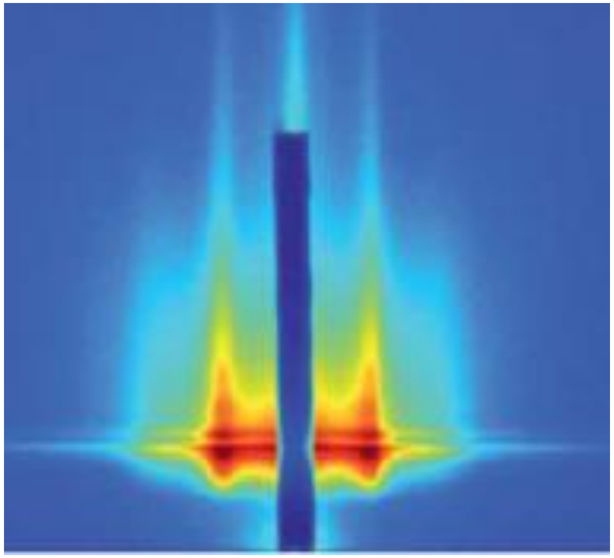

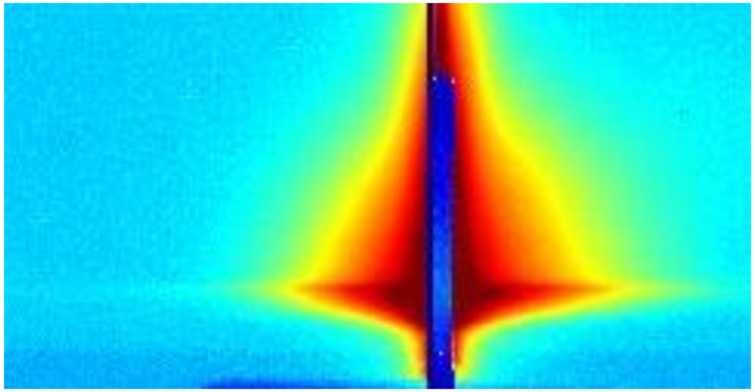

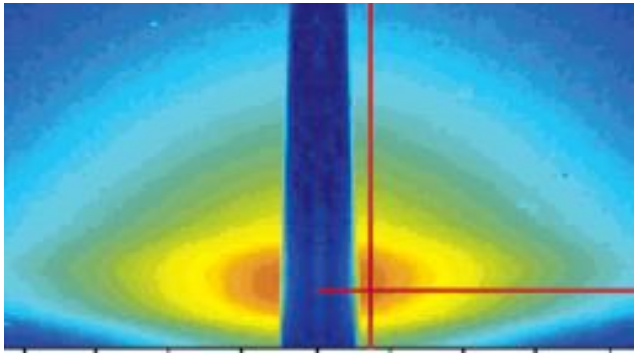

X-ray waveguide

- Type 1: with a cap layer
  - High-electron density Layer/low-electron density layer/high-electron density layer
  - Potential well in the low-electron density layer
- Type 2: without cap
  - Air/low-electron density layer/x-ray mirror
  - Quasi potential well in the low-electron density layer

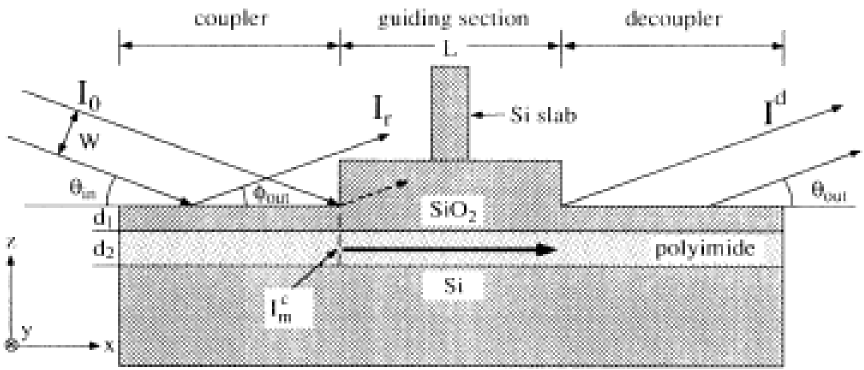

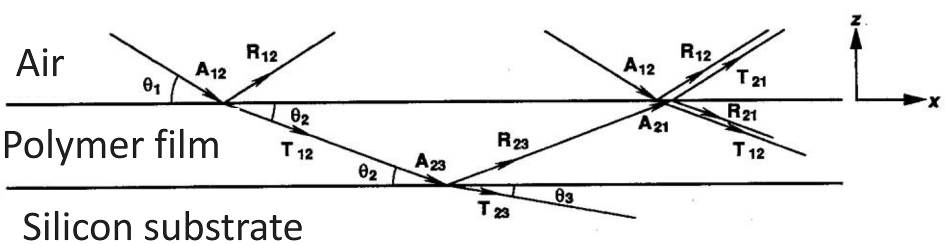

Waveguide (X-ray standing wave effect) effect

- Analogy to microwave/radio wave cavity
- X-ray standing waves generated by the mirror in the low-electron density layer
- Strong electric field intensity enhancement at “resonant” angles
- Multiple enhancement modes

Reflectivity from a 100nm polymer film on silicon

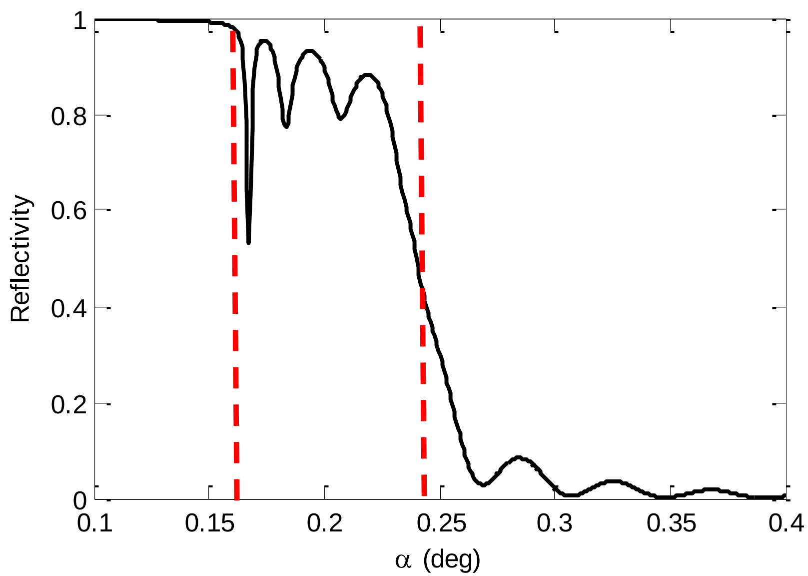

Film α_c Substrate α_c

Electric field intensity (EFI)

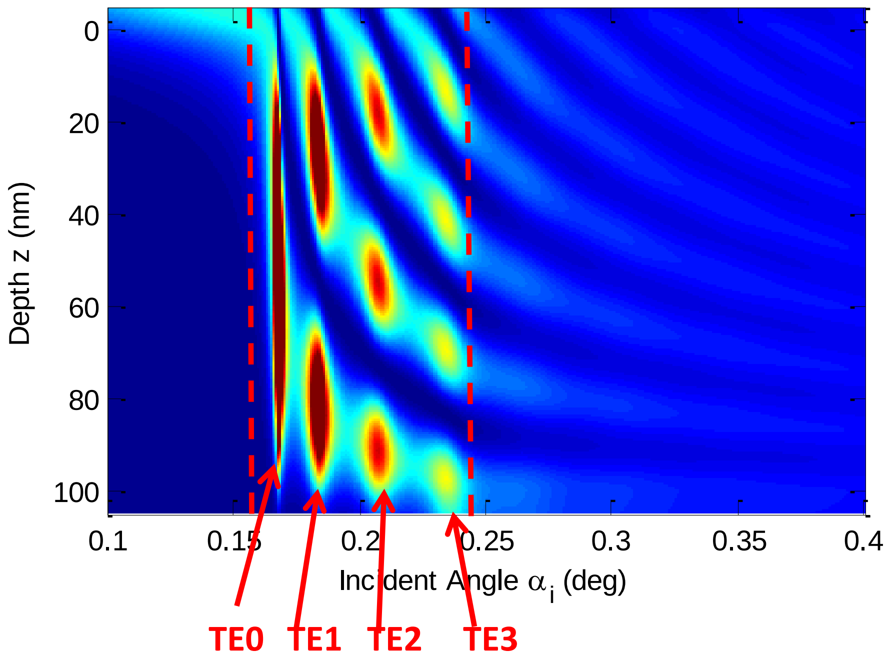

Transverse Electric (TE) mode (**resonant angles**)

Calculation of the depth dependent EFI

Parratt's Recursion

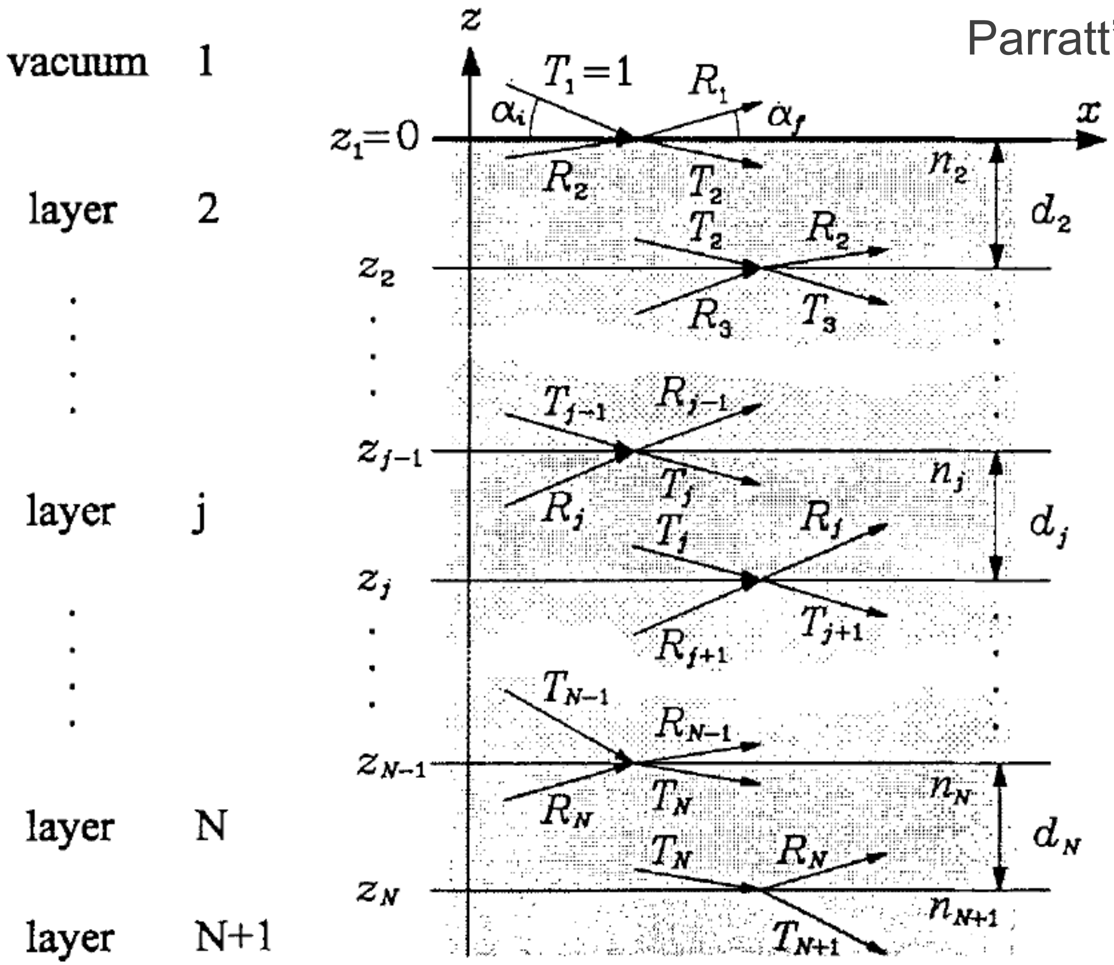

$$E_j(\boldsymbol{r},\boldsymbol{k}) = E_0 e^{-i\boldsymbol{k}_{\|}\cdot\boldsymbol{r}_{\|}}\left(T_j e^{-ik_{z,j}z} + R_j e^{ik_{z,j}z}\right)$$

What to do with depth dependent EFI?

- ✗ Only those illuminated region (high EFI) contribute to the scattering.
- ✓ It is possible to solve "3D" structure of the thin films using the waveguide effect.
  - Electric field heterogeneity provides a nano-probe in the 3rd dimension.
- Many experiments have demonstrated the signature of the effects over the years.
  - Along with the proposal of solving the structure (form factors, location).
  - Mostly happened in polymer thin films
- Solving the problem had been very challenging:
  - The thin film itself is part of the x-ray optics and changes the EFI
  - Nanostructure form factor has a different definition

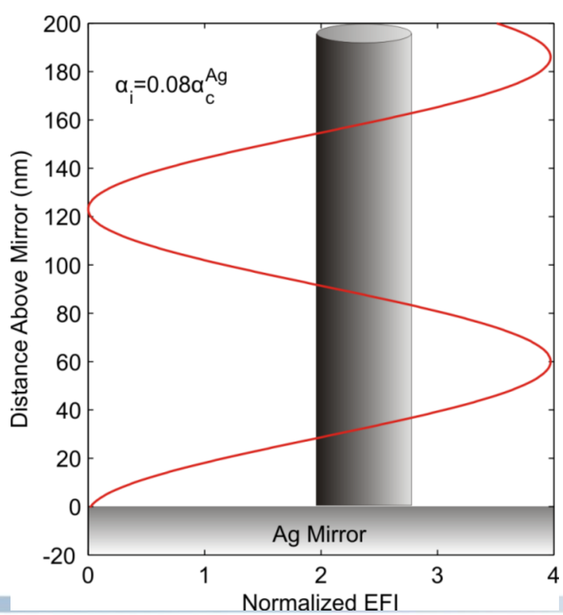

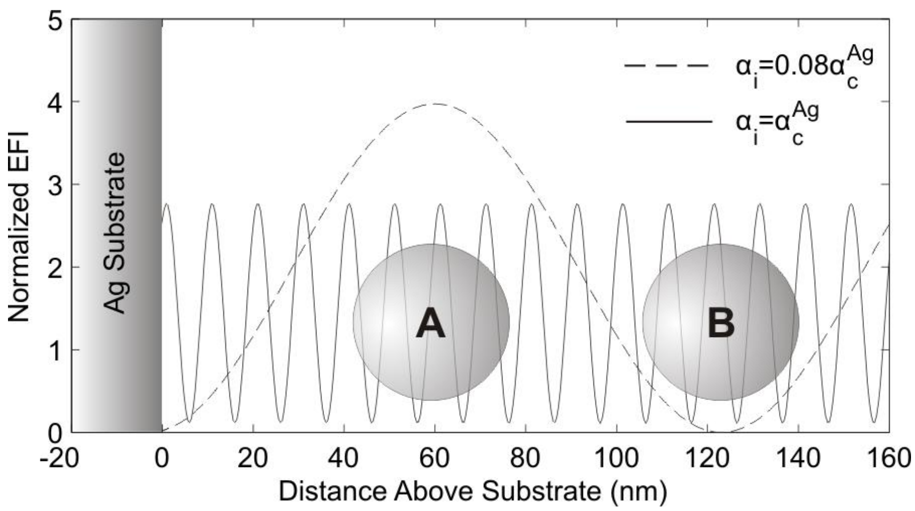

Z. Jiang et al, PRB 84, 75400 (2011)

Multilayer DWBA

- Vertical electron density profile obtained from reflectivity
- Use depth dependent reflection and transmission coefficients for form factor and structure factor

$$F\left(q_\parallel, k_z^i, k_z^f\right) = \int d\vec{r}_\parallel e^{-i\vec{q}_\parallel \cdot \vec{r}_\parallel} \int_0^d dz\, \delta\left(\vec{r}_\parallel, z\right) \sum_{m=1}^{4} D_m(z) e^{-iq_{mz}(z) z}$$

$$\text{Kronecker delta: } \delta\left(\vec{r}_\parallel, z\right) = \begin{cases} 0, & \text{outside particle} \\ 1, & \text{inside particle} \end{cases}$$

$$\begin{aligned} q_{1z}(z) &= k_z^f(z) - k_z^i(z) \\ q_{2z}(z) &= -k_z^f(z) - k_z^i(z) \\ q_{3z}(z) &= -q_{2z}(z) \\ q_{4z}(z) &= -q_{1z}(z) \end{aligned}$$

$$\begin{aligned} D_1(j) &= T_j^i T_j^f \\ D_2(j) &= T_j^i R_j^f \\ D_3(j) &= R_j^i T_j^f \\ D_4(j) &= R_j^i R_j^f \end{aligned}$$

Parratt's Recursion:

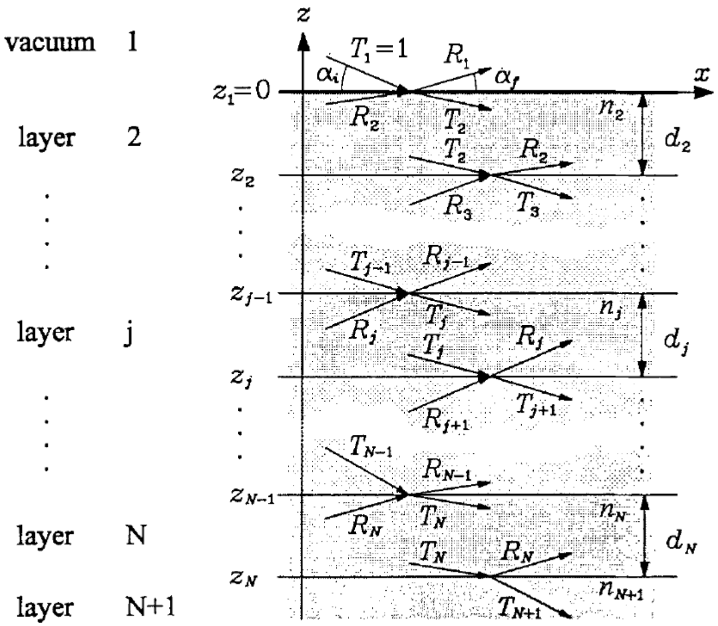

- For very large angles

$$D_1 = 1,\ D_{2,3,4} = 0$$

$$F\left(q_\parallel, k_z^i, k_z^f\right) = \int d\vec{r}_\parallel e^{-i\vec{q}_\parallel \cdot \vec{r}_\parallel} \int_0^d dz\, \delta\left(\vec{r}_\parallel, z\right) e^{-iq_z z} = F(q)$$

Born Approximation

Slicing of particles or structures inside the Layer

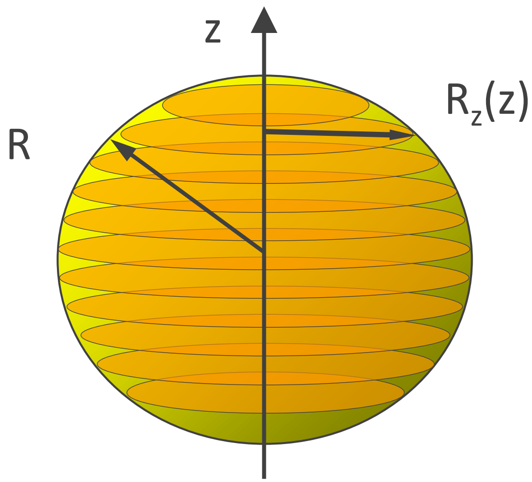

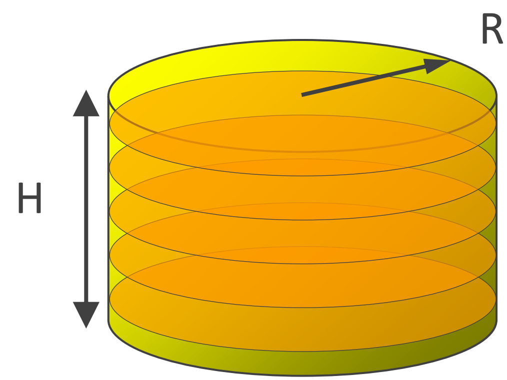

$$F\left(q_\parallel,k_z^i,k_z^f\right)=\frac{2\pi}{q_\parallel}\int_0^R dz R_z(z) J_1\left[q_\parallel R_z(z)\right]\sum_{m=1}^{4} D_m(z) e^{-iq_{mz}z}$$

Large angle

$$F(q)=4\pi R^3\frac{\sin(qR)-qR\cos(qR)}{(qR)^3}e^{-iq_zR}$$

Small particle

$$F\left(q_\parallel,k_z^i,k_z^f\right)=\sum_{m=1}^{4} D_m(z) F\left(q_\parallel,q_{mz}\right)$$

$$F\left(q_\parallel,k_z^i,k_z^f\right)=\frac{2\pi}{q_\parallel}\int_0^H dz R J_1\left[q_\parallel R\right]\sum_{m=1}^{4} D_m(z) e^{-iq_{mz}z}$$

Large angle

$$F(q)=2\pi R^2 H\frac{J_1\left[q_\parallel R\right]}{q_\parallel R}\frac{\sin(q_zH/2)}{q_zH/2}e^{-iq_zH/2}$$

Small particle

$$F\left(q_\parallel,k_z^i,k_z^f\right)=\sum_{m=1}^{4} D_m(z) F\left(q_\parallel,q_{mz}\right)$$

Model comparison (spherical nanoparticle)

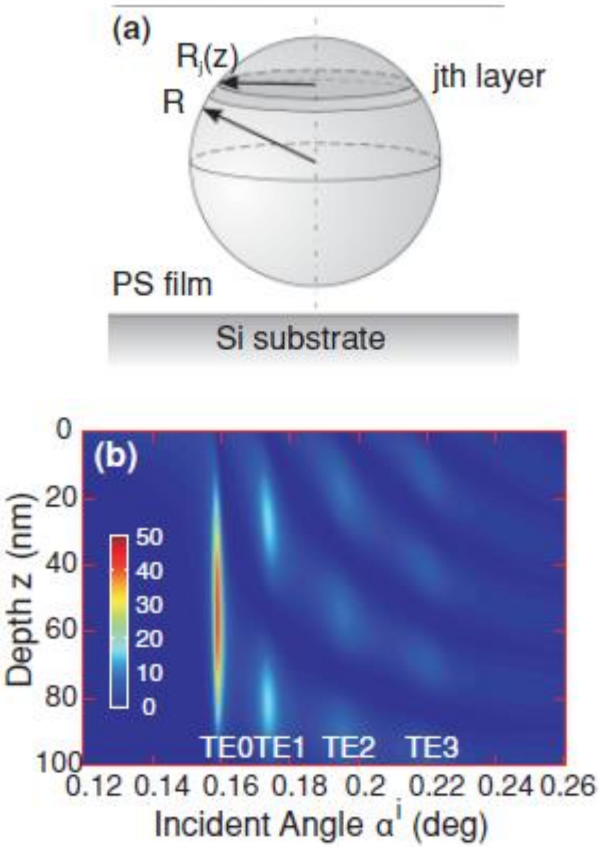

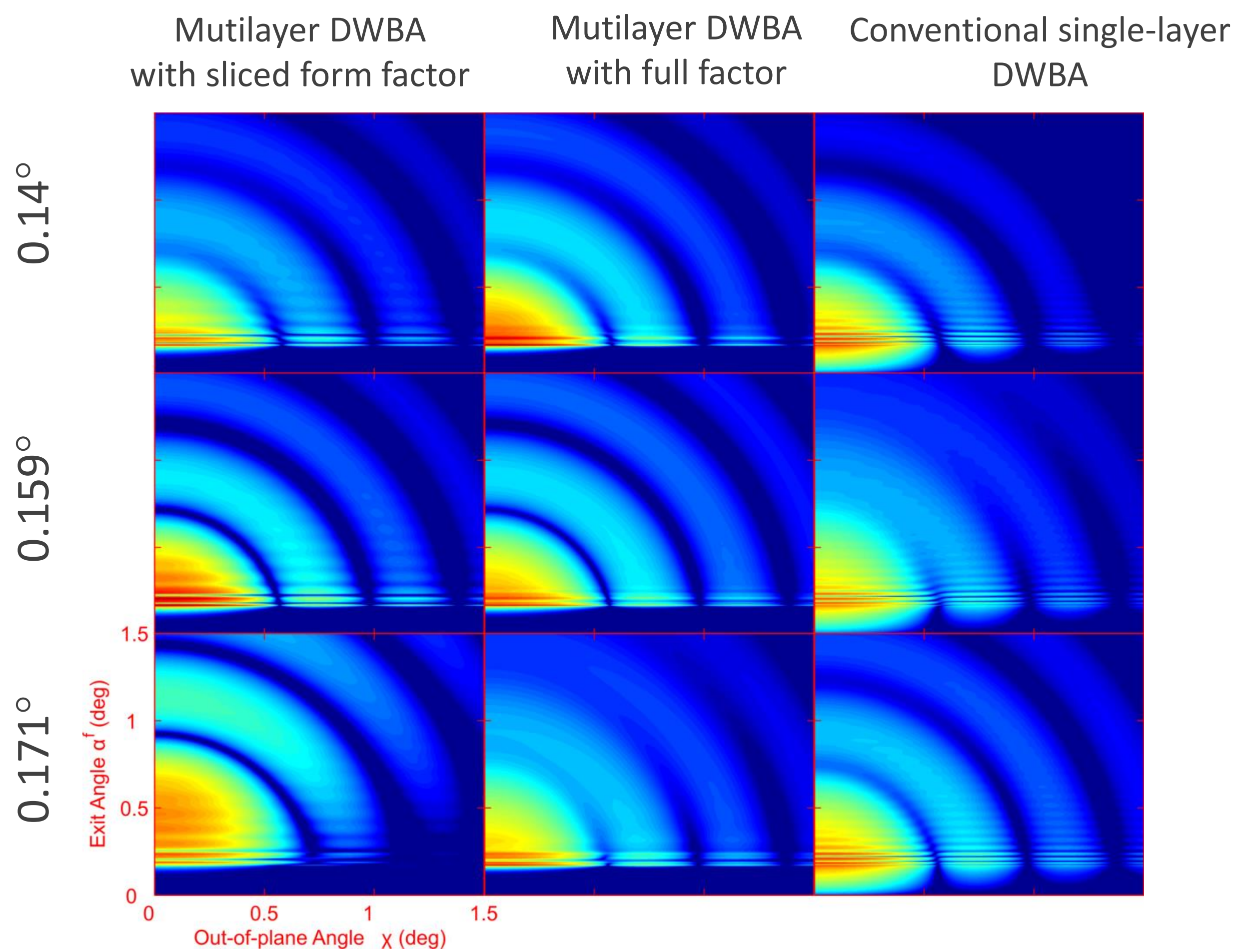

- The scattering intensity is altered for both above and near the critical angles.
- At the 2nd resonant angle (0.171°), the sphere can be viewed as a stack two objects of much smaller size due to the EFI effect. This leads to the significant high-end shift of the overall form factor oscillations.
- *The slicing model can provide more accurate description of the form factor and depth profile.*

Z. Jiang et al, PRB 84, 75400 (2011)

Sandwiched film of polymer-nanoparticle composite

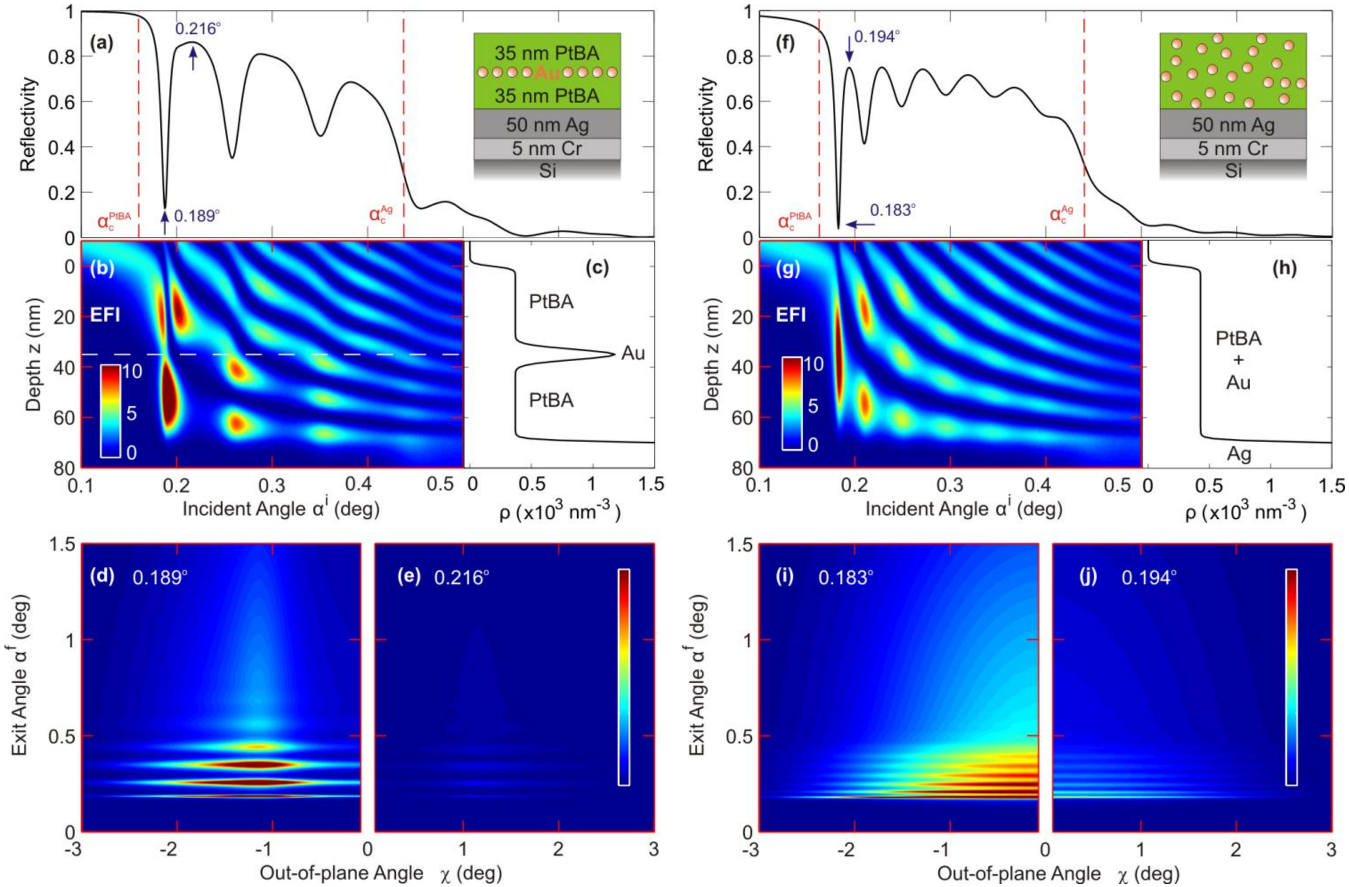

- The redistribution of the gold nanoparticles changes the XSW modes; this has been experimentally confirmed.
- The wave-guide enhancement at certain incident angles has been used to solve real problems, such as kinetics of the anisotropic diffusion of nanoparticles thin films, and the dynamics of these buried nanoparticle/polymer interface.

S. Narayanan, et al, PRL, 94, 145504 (2005); D. R. Lee, et al, APL. 88, 153101 (2006); S. Narayanan, et al, PRL, 98, 185506 (2007)

Self-directed self-assembly of nanoparticle/copolymer

- PS-b-P2VP/gold nanoparticle composite film
- 75 nm thick film of PS-b-P2VP (PS: 102 kg/mol, P2VP: 97 kg/mol)
- 10 wt-% of mono-disperse gold nanoparticles (R=2.15 nm)
- Solvent annealed in dichloromethane for 12 hrs followed by thermal annealing at 170°C in vacuum for 30 min.
- Vertical lamella; gold in P2VP phase (surface or interior?).

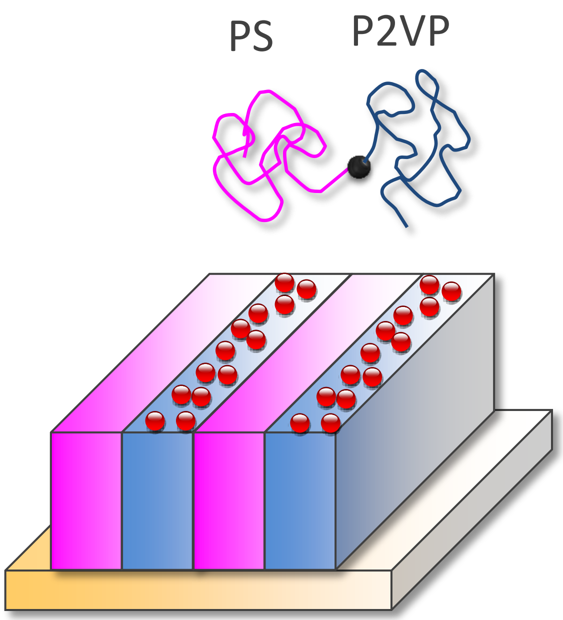

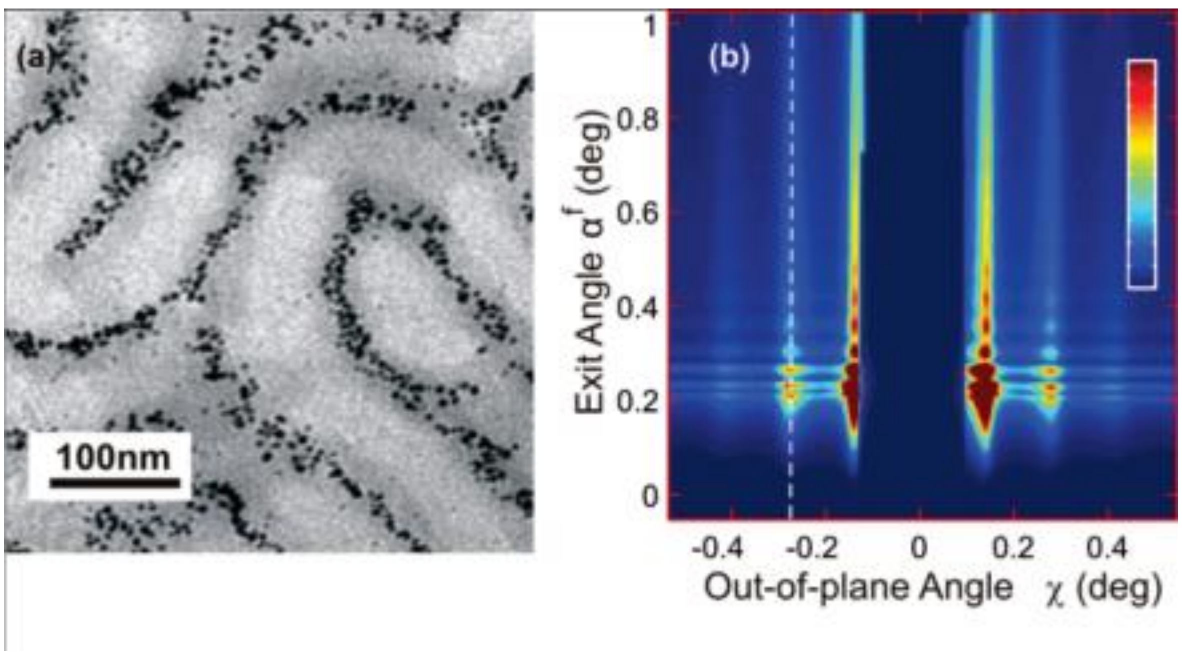

Self-directed self-assembly of nanoparticle/copolymer

- Solvent (dichloromethane) annealing followed by thermal annealing drives nanoparticles to the surface
- stand-up lamellar structures.

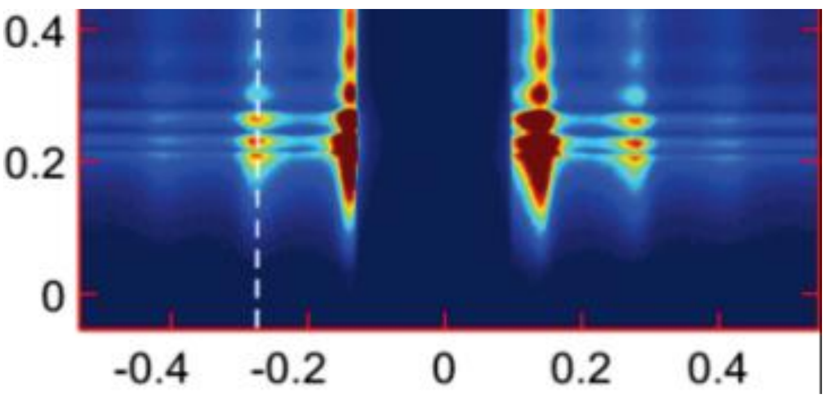

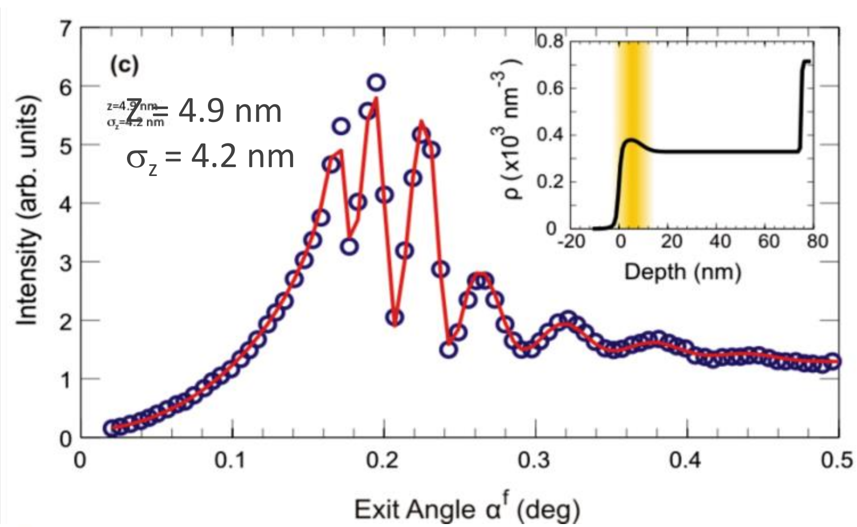

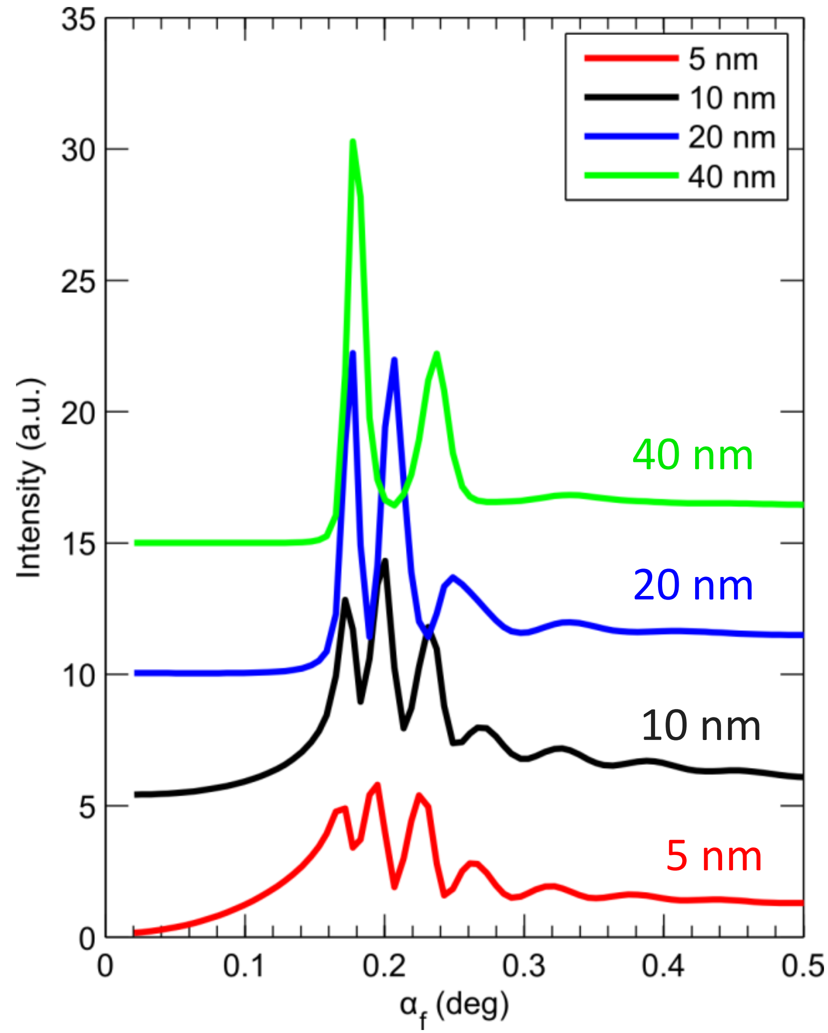

Z. Jiang et al, PRB 84, 75400 (2011)

Supported (exposed) dense nano-objects

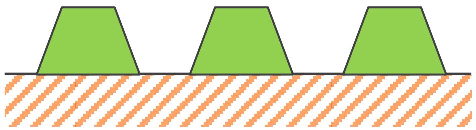

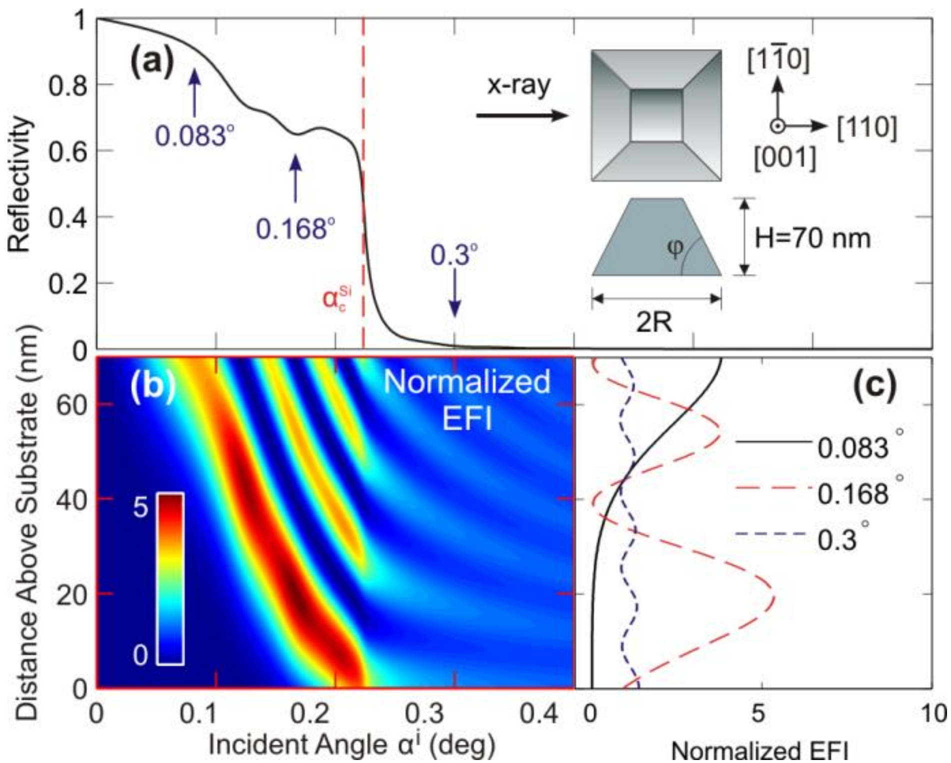

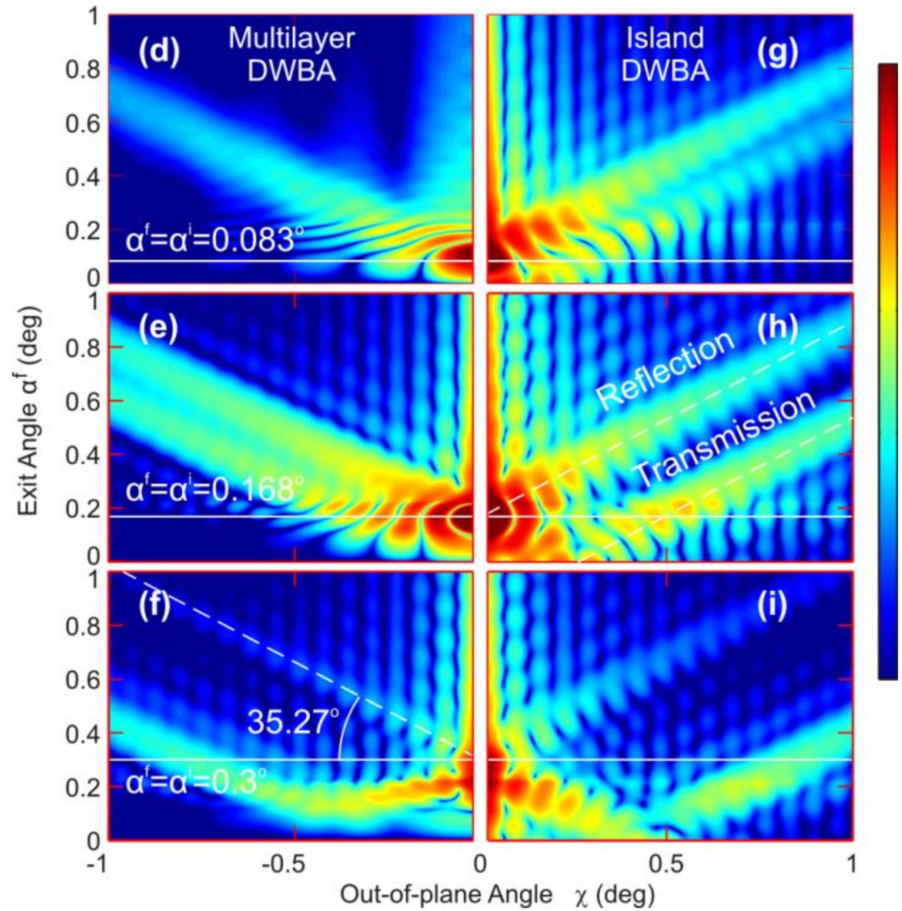

Z. Jiang et al, PRB 84, 75400 (2011)

More GISAXS references

- DWBA fundamental (single rough interface)
  - Sinha, et al., Phys. Rev. B 38, 2297 (1988)
- Multiple rough interfaces
  - Holy et al., Phys. Rev. B 47, 15896 (1993); 49, 10668 (1994)
- Supported nano-objects
  - Rauscher et al, J. Appl. Phys. 86, 6763 (1999) (IsGISAXS)
  - Lazzari, J. Appl. Cryst. 35, 406 (2001)
- Nanostructures in supported single layer film
  - Lee et al.,, Macromolecules 38, 3395 and 4311 (2005)
  - Tate et al., J. Phys, Chem. B 110, 9882 (2006)
- Depth-dependence structures in films
  - Babonneau et al., Phys. Rev. B 80, 155446 (2009)
  - Jiang, et al., Phys. Rev. B 84, 075440 (2011)
- Some GISAXS analysis softwares
  - IsGISAXS, FitGISAXS, BornAgain, HipGISAXS

Appendix: general GISAXS interpretation

General interpretation of GISAXS data

- Nanostructure morphology
  - Form factor *F*: size, shape, facet etc.
  - Structure factor *S*: inter-particle correlation
- General rule: scattering intensity $I \sim |F|^2 S$ (for both SAXS and GISAXS)
- Separation of form factor and structure factor
  - Diluted or disordered systems, the inter-particle correlation is weak, i.e., the interference function is nearly one
  - Concentrated system, particles are strongly correlated at small q values.
  - Quick analysis is not accurate.
  - To help model the data, experimentally one needs to measure
    - away from the origin of the reciprocal space, i.e. high q
    - over several orders of magnitude in q (with clean background)

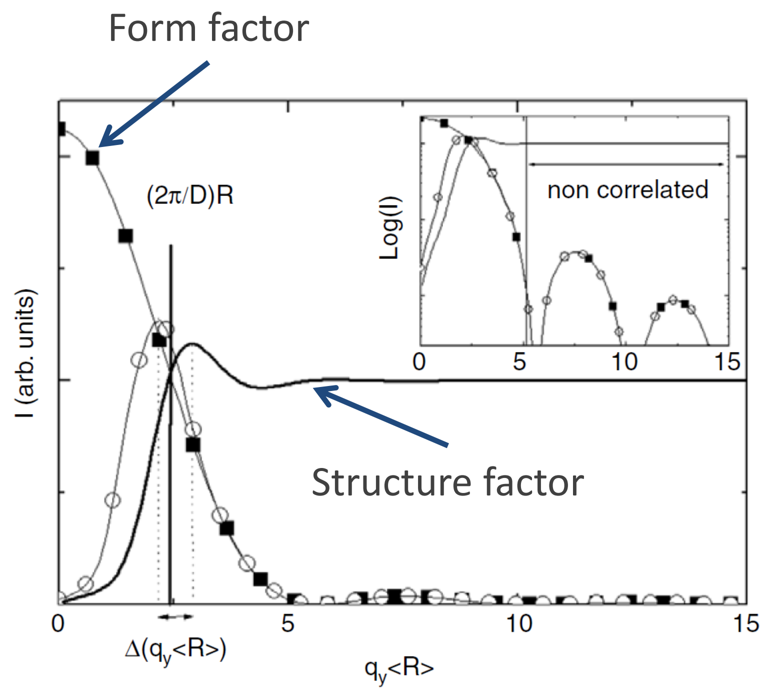

In-plane linecut (q_y) for disordered vertical cylinders on a substrate

Form factor

- The Fourier transform of the shape (electron density distribution)

$$\int \rho(\boldsymbol{r}) e^{i\boldsymbol{Q}\cdot\boldsymbol{r}} d\boldsymbol{r}$$

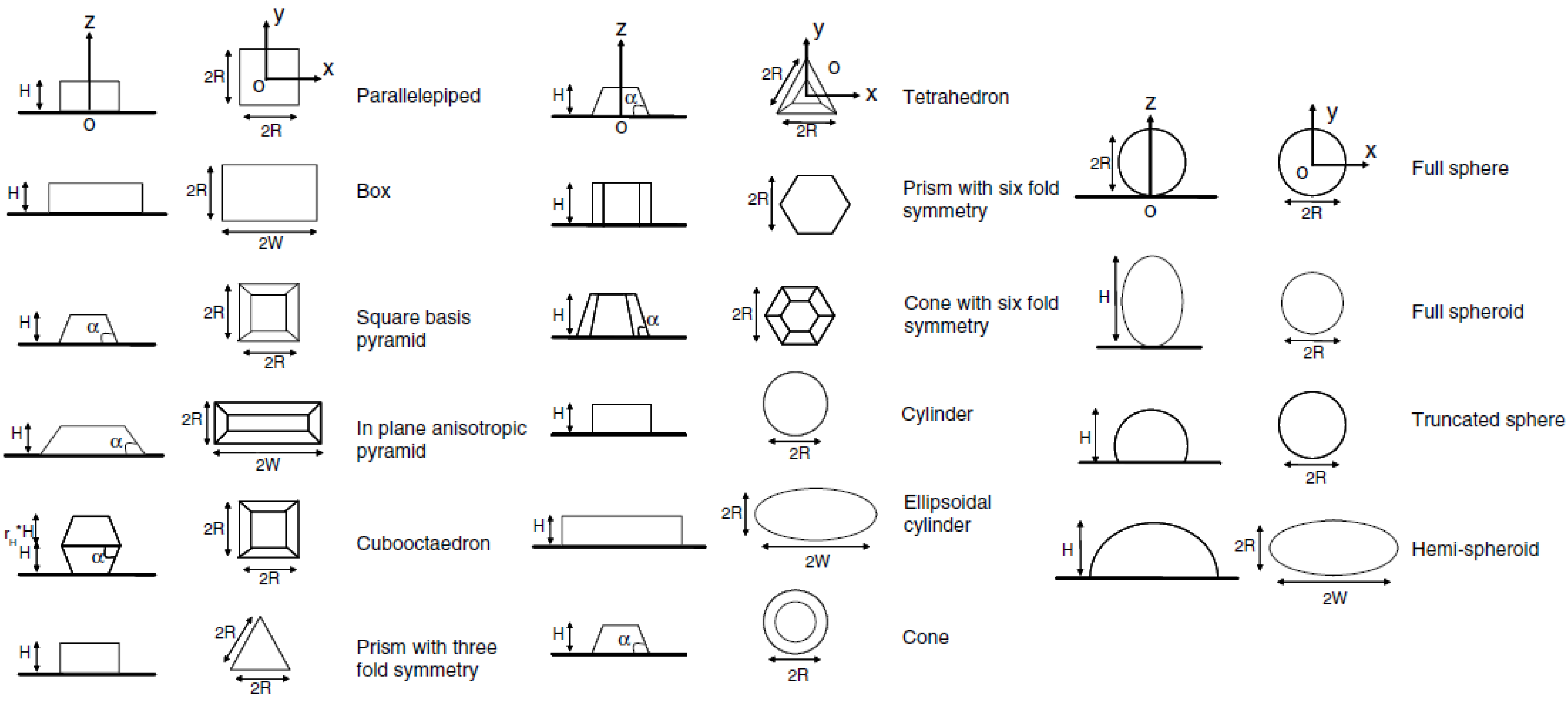

Renaud's GISAXS review paper

Form factor - facets

- For an anisotropic nanostructure like one with facets and edges, the form factor depends on its orientation with respect to the x-ray beam.
  - Incident x-ray along a facet
  - Incident x-ray along an edge

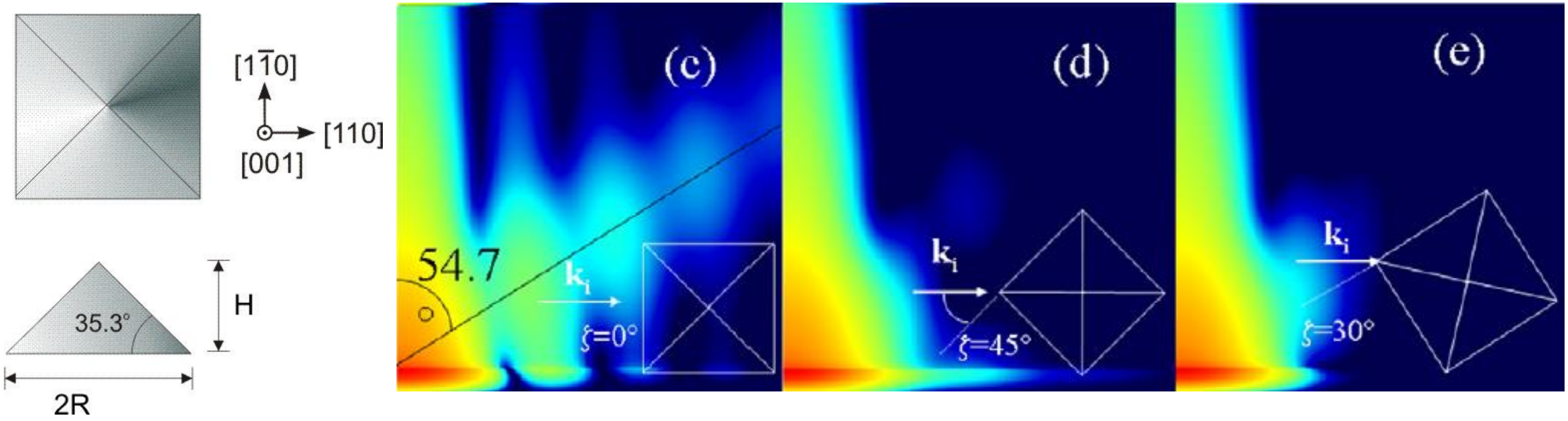

- Pyramid-like nanocrystals of fcc material on a (001) surface. The main side facets are (111) making an angle of 35.3° with respect to the surface
- When x-ray is incident along a face, pronounced scattering rods by facets appear at a scattering angle corresponding to the facet angle — CRT (crystal truncation rod). At other rotation ζ angles, the rods become less intense.
- GIXS as a function of rotation can be used to for quick determination of the symmetry of nanocrystals as well as facet angles.

Form factor - polydisperse structures

- Small polydispersity: nanostructures are close in shape and size; the dip (zero) positions of the form factor indicate the nanostructure parameters like size and shape.
- Large polydispersity in size and shape is a nature consequence of the growth-coalescence process such as MBE (molecular beam epitaxy).
  - Depending on the growth kinetics, the size distribution is hard to determine precisely. However, a *lognormal distribution* is often used.
  - Asymptotic behavior of the form factor at high q, i.e., $I \sim q^{-n}$, can be used to determine the shape of the nanostructure — *Porod approach* often used in SAXS.

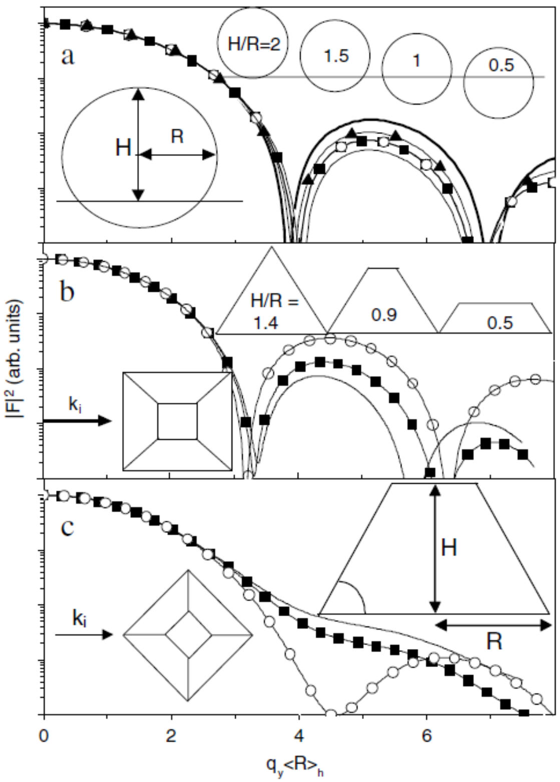

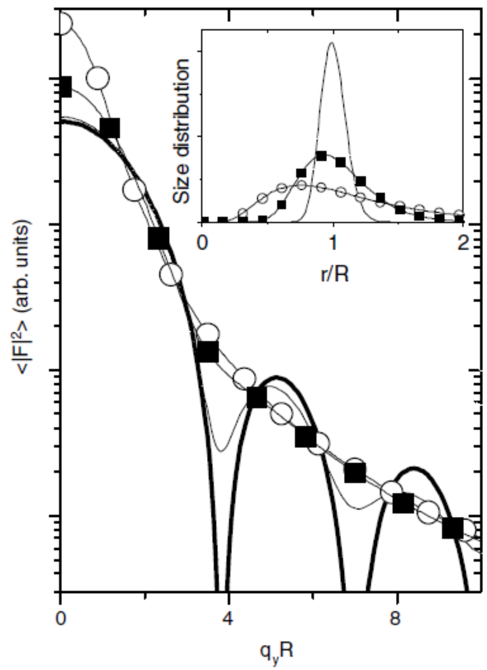

Vertical cylinders with lognormal distribution in radius

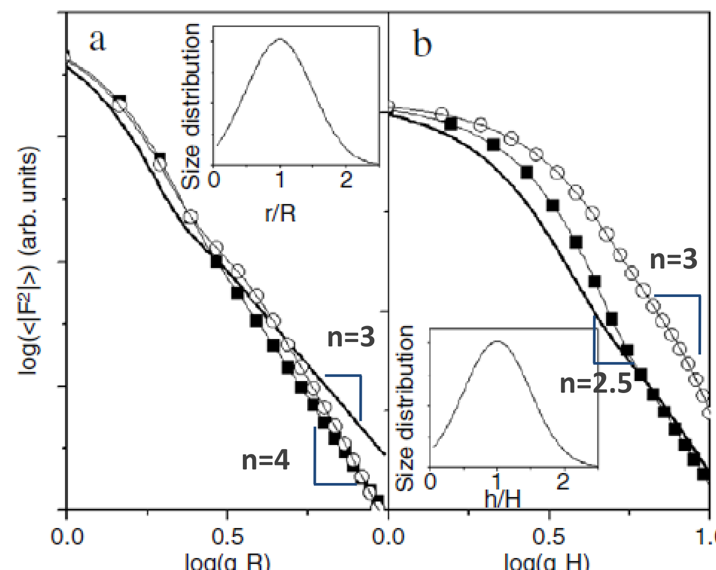

Asymptotic behavior for cylinder H/R=1 (solid line), hemisphere (square), and pyramid H/R=0.9 and ζ=0 (circles)

Structure factor

- For non-periodic (non-crystal) structures, the particle position (i.e., inter-particle correlation or interference function) is often described statistically. Common models are
  - Percus-Yevick approximation for hard spheres in 3D (Kinning and Thomas, Macromolecules, 17, 1712 (1984))

$$S(q_\parallel, q_z) = \frac{1}{1 + 24\eta G(2qR)/(2qR)}$$

$$\begin{aligned} G(x) = {} & \frac{\alpha}{x^2}(\sin x - x\cos x) \\ & + \frac{\beta}{x^3}\left[2x\sin x + (2 - x^2)\cos x - 2\right] \\ & + \frac{\gamma}{x^5}\{-x^4\cos x + 4[(3x^2 - 6)\cos x \\ & + (x^3 - 6x)\sin x + 6]\}, \end{aligned}$$

$$\alpha = (1 + 2\eta)^2/(1 - \eta)^4,$$
$$\beta = -6\eta(1 + \eta/2)^2/(1 - \eta)^4,$$
$$\gamma = \eta\alpha/2.$$

η is the volume fraction

  - 1D or 2D paracrystal model for 2D structures on a surface (Vainshtein, *Diffraction of X-rays byChain Molecules*, Chap. V)

$$S(q_\parallel, q_z) = \frac{1 - e^{-q_\parallel^2\sigma_d^2}}{1 + e^{-q_\parallel^2\sigma_d^2} - 2e^{-q_\parallel^2\sigma_d^2/2}\cos(q_\parallel d)}$$

d is the nearest-neighbor distance and σ_d is its root-means-square deviation

- In many cases, the interaction potential are unknown and can neither be predicted thermodynamically due to the highly non-equilibrium growth kinetics. It is thus often useful to resort to an ad hoc interference function deduced from other measurement such as plane view TEM, SEM or AFM.

Separation of form factor and structure factor for polydispersed structures

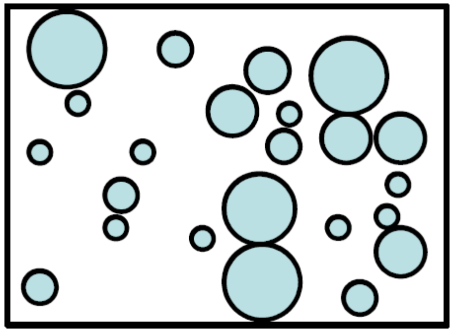

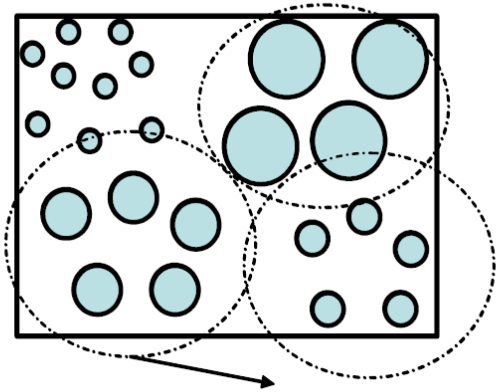

- DA (Decoupling approximation): the kind (size, shape etc) of particles and their relative location are not correlated.

$$\left(\frac{d\sigma}{d\Omega}\right) \cong \underbrace{\left(\langle |F(\boldsymbol{q})|^2\rangle - |\langle F(\boldsymbol{q})\rangle|^2\right)}_{\text{Diffuse part to account for the disorder of the particle nature (size, shape)}} + |\langle F(\boldsymbol{q})\rangle|^2 S(\boldsymbol{q})$$

- LMA (local monodisperse approximation): the particle collection is made of monodisperse domains which size are larger than the coherence length of the x-ray beam. The total scattering intensity is obtained by an incoherent sum of the intensities from each domain.

$$\left(\frac{d\sigma}{d\Omega}\right) \cong \langle |F(\boldsymbol{q})|^2\rangle S(\boldsymbol{q})$$

Example – 1nm thick Pd nanocrystals on MgO(001)

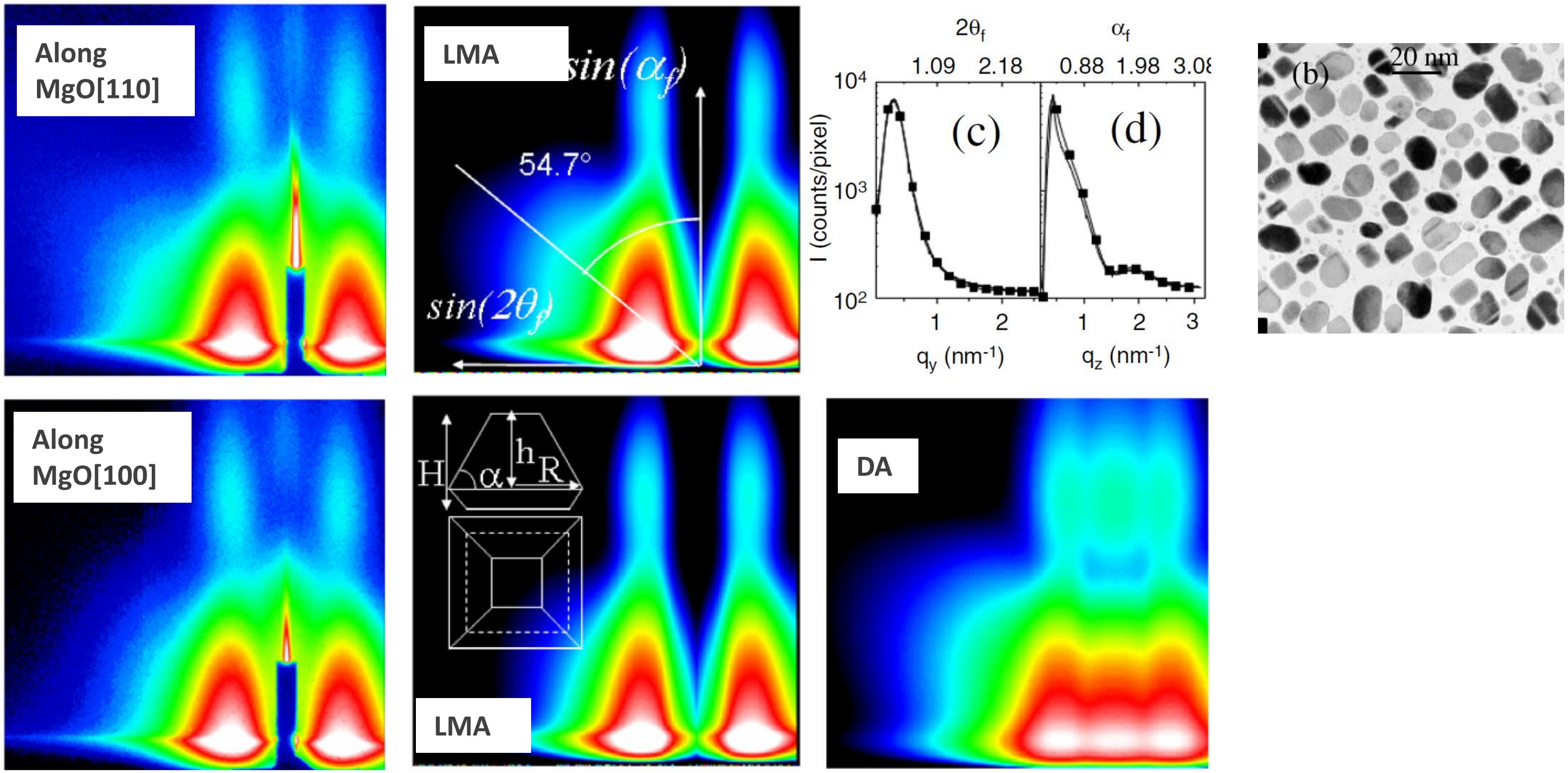

Revenant et al., PRB 69, 35411 (2004)

- MBE Pd islands have a shape of truncated octahedron with a square base.
- Neither LMA nor DA can correctly reproduce the diffuse scattering close to the beam stop (small q). This is due to the ignorance of the long-range size-position or size-size coupling.

In-situ monitoring of the nanocrystal growth

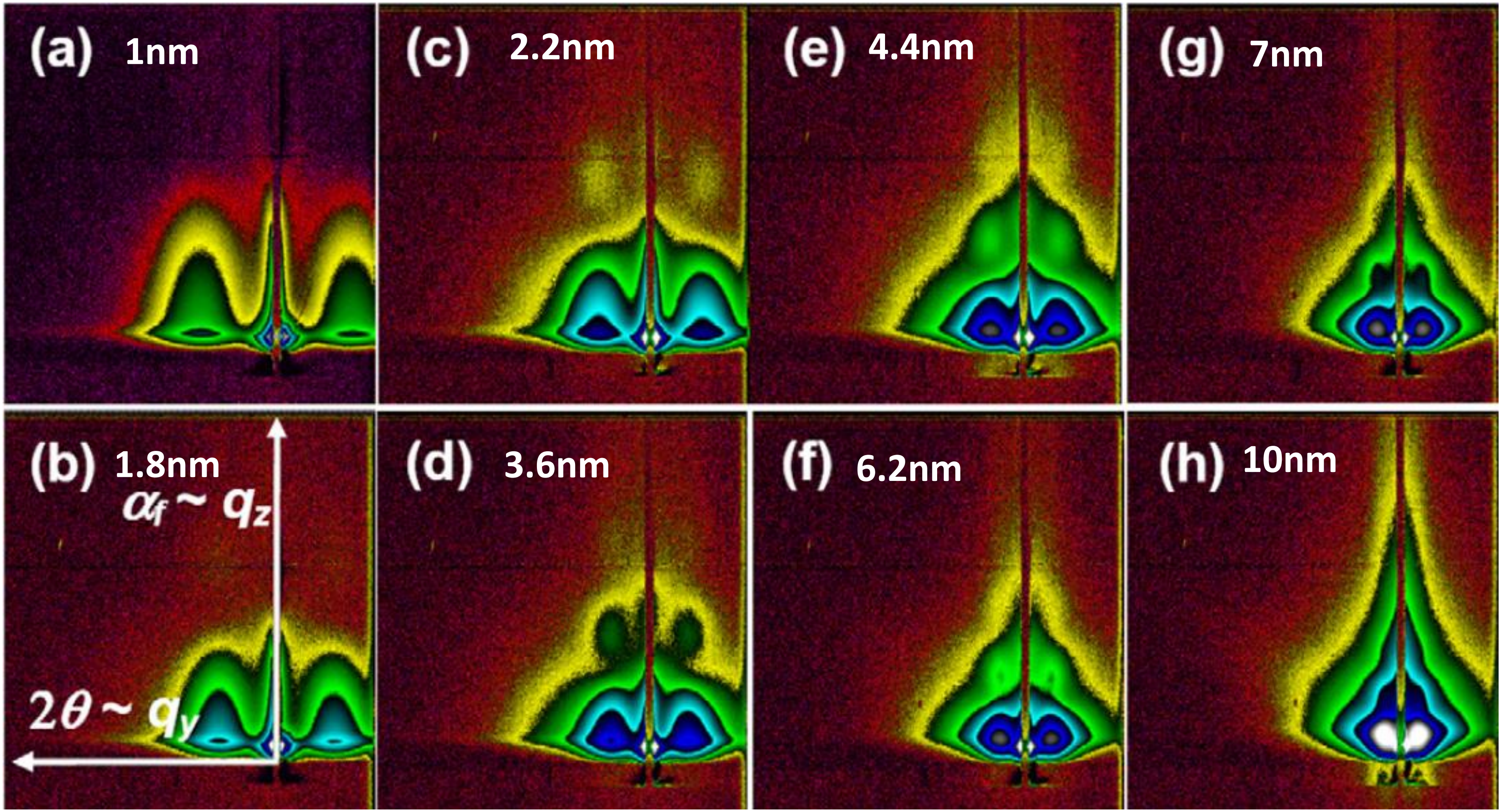

- Growth of Ag nano-island on MgO(001) surface. Beam is incident along MgO[100]
- Quantitative analysis of the GIXS pattern during the growth gives information about the change nanocrystal size, shape as well as orientations

Revenant et al., PRB, 79, 1 (2009)

Self-assembled Ge islands on Si (111) substrate

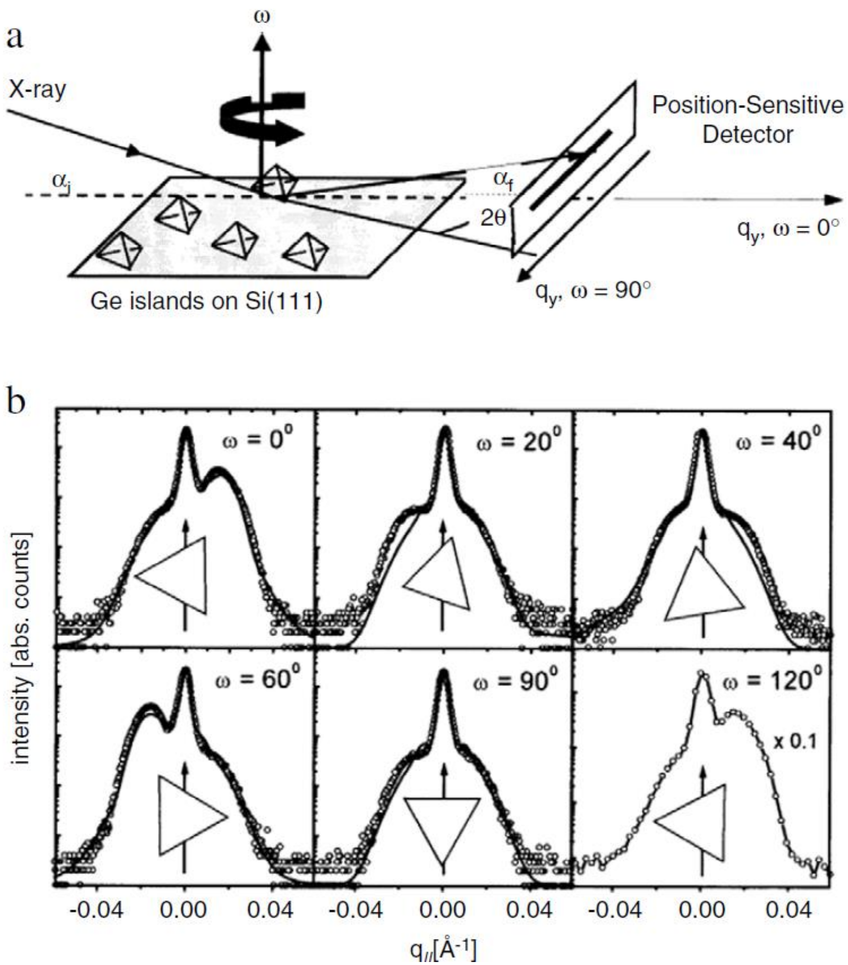

- GISAXS measurements with various in-plane rotation angle clearly shows a 3-fold symmetry of the Ge islands, which cannot be determined by transmission SAXS.

Metzger, et al., Thin Solid Films 336, 1 (1998)

Appendix:3D structure indexing

Revisiting Ewald sphere

- Diffraction occurs when Laue condition is fulfilled

$$\boldsymbol{q} = \boldsymbol{G}$$

$\boldsymbol{q} = \boldsymbol{k}' - \boldsymbol{k}$: wave vector transfer
$\boldsymbol{G}$: reciprocal lattice vector

- Ewald sphere construction
  - Draw a sphere with radius $|k|$ centered at the sample position (in the lab frame)
  - Superimpose the reciprocal space with its origin at the intersection of the incident beam and the Ewald sphere surface.
  - Reciprocal lattices falling on the sphere surface give diffractions.

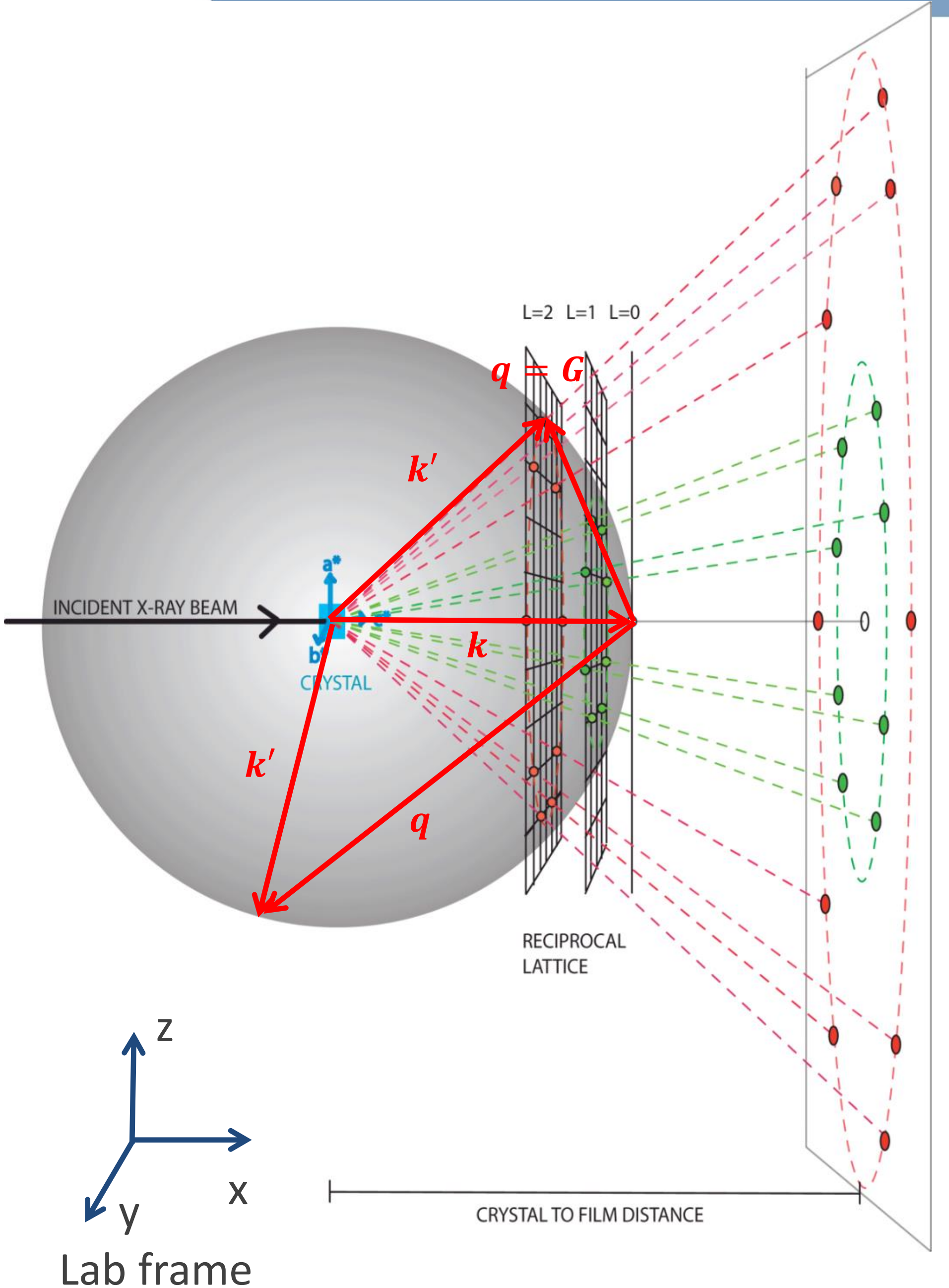

3D structure indexing in supported organized films

- Ewald sphere is defined in the lab frame; reciprocal space lattices are conveniently defined in the sample frame. The two frames are related by an incident angle dependent rotation matrix

$$R_y(\alpha) = \begin{bmatrix} \cos\alpha & 0 & \sin\alpha \\ 0 & 1 & 0 \\ -\sin\alpha & 0 & \cos\alpha \end{bmatrix}$$

- Reciprocal lattice vector in the lab frame is obtained from the sample frame through a rotation operation

$$\left(G_x, G_y, G_z\right) = R_y\boldsymbol{G} = R_y(h\boldsymbol{a}_1^* + k\boldsymbol{a}_2^* + l\boldsymbol{a}_3^*).$$

- Allowed diffractions for lattice points on Ewald sphere surface

$$\boxed{|\boldsymbol{G}_{lab} - \boldsymbol{k}|^2 - |\boldsymbol{k}|^2 = (G_x - k)^2 + G_y^2 + G_z^2 - k^2 \le \Delta G^2}$$

ΔG accounts for the finite size of Bragg peak in the reciprocal space and any mosaicity of the domains.

- Wave vector transfer (q_x, q_y, q_z) is defined in the sample frame

3D structure indexing in supported organized films

- Domains of surface supported structures often have a statistical orientation distribution with respect to surface normal. Assume the orientation is isotropic in the surface plane, which is often true for most self-assembled structures; thus the reciprocal lattice points become a set of rings (like those in power diffraction), dependent only on in-plane $q_{||} = \sqrt{q_x^2 + q_y^2}$
- Laue condition and the rotation operation of q are given by

$$\boxed{\begin{array}{c} G_x^2 + G_y^2 + G_z^2 - q_{\|}^2 + q_z^2 + q_z(G_x \sin\alpha - G_z \cos\alpha) = 0 \\ -G_x \sin\alpha + G_z \cos\alpha = q_z \end{array}}$$

- Solve the three equations simultaneously for $(q_{\|}, q_z)$. Thus the outgoing angles are

$$\alpha_f = \arcsin\sqrt{\left(\frac{q_z}{k}\right)^2 + \sin^2\alpha_i - \frac{2q_z}{k}\sqrt{n^2 - 1 + \sin^2\alpha_i}}$$ Exit angle (reflection)

$$\alpha_f = \arcsin\sqrt{\left(\frac{q_z}{k}\right)^2 + \sin^2\alpha_i + \frac{2q_z}{k}\sqrt{n^2 - 1 + \sin^2\alpha_i}}$$ Exit angle (transmission)

$$2\theta = \arccos\left(\frac{\cos^2\alpha_f + \cos^2\alpha_i - (q_{\|}/k)^2}{2\cos\alpha_f \cos\alpha_i}\right)$$ In-plane angle

- Softwares: NanoCell (Mathematica, Hillhouse at Washington U.) and GIXSGUI (Matlab, 8ID/APS/ANL)

3D structure indexing - example #1

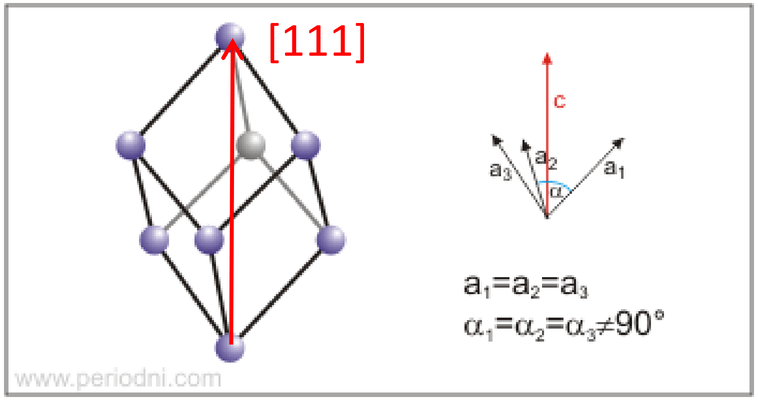

- Rhombohedral nanoporous silica thin film with R-3m symmetry, a=114 A and α=87°
- [111] direction perpendicular to the silicon substrate
- E=7.35 KeV, and incident angle is 0.23°
- Born approximation does not work well when exit angle is close to the critical angle.
- Born approximation does not predict some peaks which arises from the transmitted and reflected scattering channels.

M. Tate et al., JPCB 110, 9882 (2006)

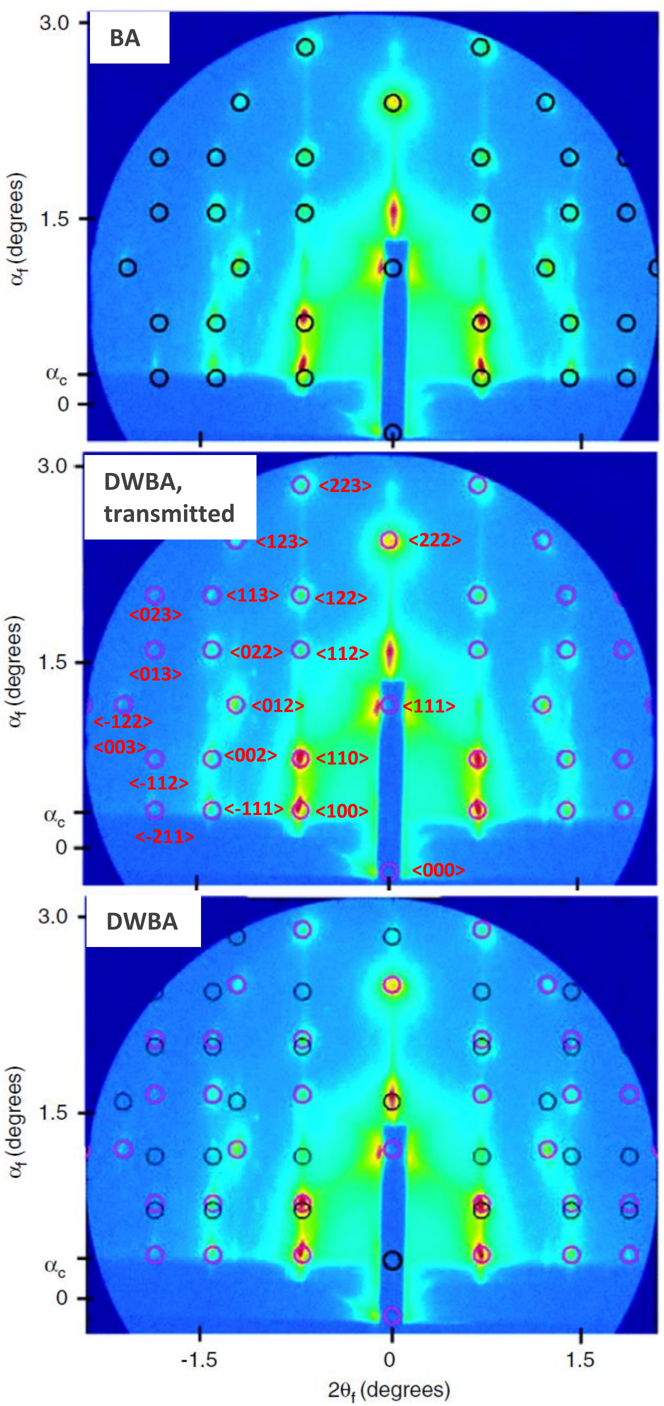

3D structure indexing - more examples

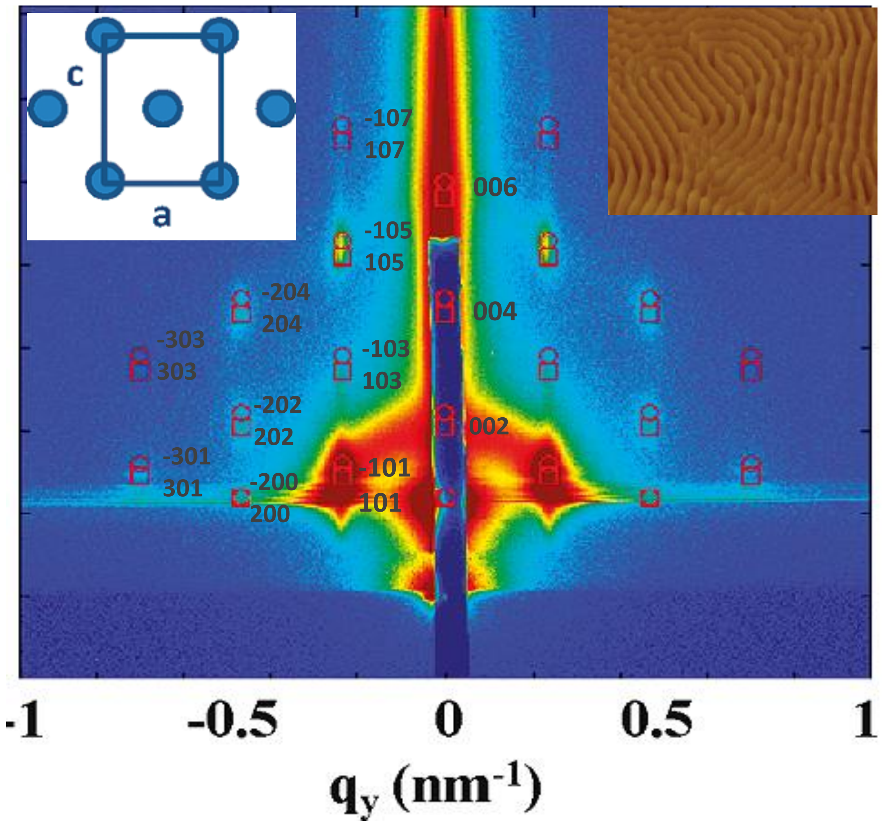

Hexagonally closely packed (HCP) cylinders self-assembled in PtBMA-PMMA block-copolymer films
Y. Sun, et al., Macromolecules 44, 6525 (2011)

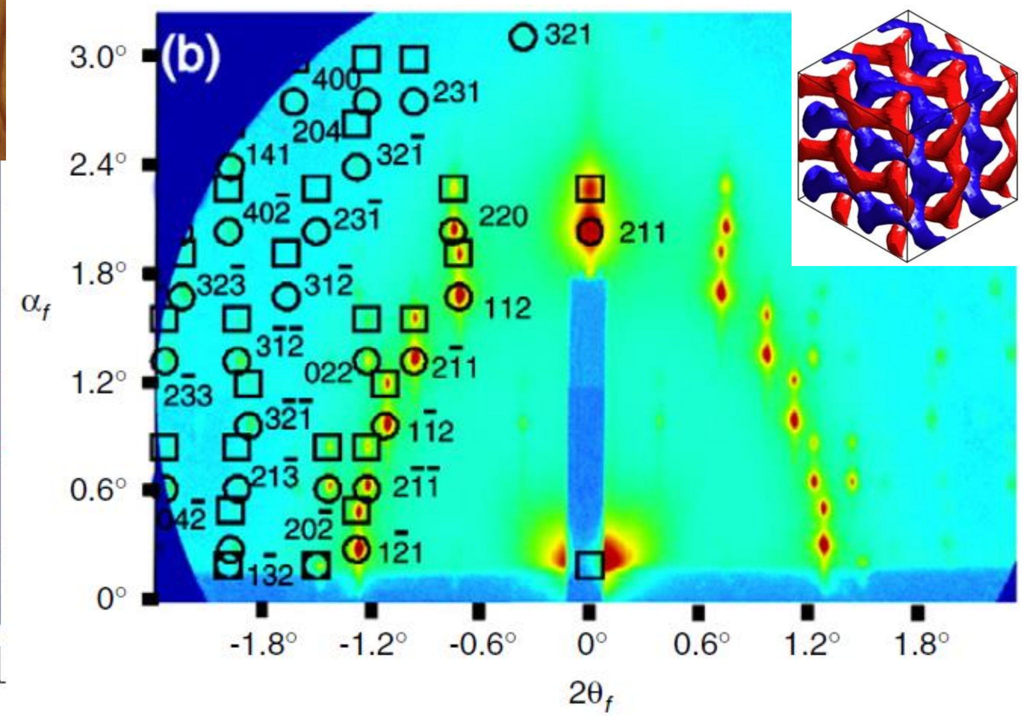

Double-gyroid porous film on FTO substrate
V. Urade et al., Chem. Mater. 19, 768 (2007)